

# Decay $\phi(1020) \rightarrow \gamma f_0(980)$ : analysis in the non-relativistic quark model approach

A.V. Anisovich, V.V. Anisovich, V.N. Markov,  
V.A. Nikonov, and A.V. Sarantsev

May 10, 2019

## Abstract

We demonstrate the possibility of a good description of the processes  $\phi(1020) \rightarrow \gamma\pi\pi$  and  $\phi(1020) \rightarrow \gamma f_0(980)$  within the framework of non-relativistic quark model assuming  $f_0(980)$  to be dominantly quark–antiquark system. Different mechanisms of the radiative decay, that is, the emission of photon by the constituent quark (additive quark model) and charge-exchange current, are considered. We also discuss the status of the threshold theorem applied to the studied reactions, namely, the behaviour of the decay amplitude at  $M_{\pi\pi} \rightarrow m_\phi$  and  $m_{f_0} \rightarrow m_\phi$ . In conclusion the arguments favouring the  $q\bar{q}$  origin of  $f_0(980)$  are listed.

## 1 Introduction

The  $K$ -matrix analysis of meson spectra [1, 2, 3] and meson systematics [4, 5] point determinately to the quark-antiquark origin of  $f_0(980)$ . However there exist hypotheses where  $f_0(980)$  is interpreted as four-quark state [6],  $K\bar{K}$  molecule [7] or vacuum scalar [8]. The radiative and weak decays involving  $f_0(980)$  may be decisive tool for understanding the nature of  $f_0(980)$ .

In the present paper the reaction  $\phi(1020) \rightarrow \gamma f_0(980)$  is considered in terms of non-relativistic quark model assuming  $f_0(980)$  to be dominantly the  $q\bar{q}$  state. Non-relativistic quark model is a good approach for the description of the lowest  $q\bar{q}$  states of pseudoscalar and vector nonets, so one may hope that the lowest scalar  $q\bar{q}$  states are described with reasonable accuracy as well. The choice of non-relativistic approach for the analysis of the reaction  $\phi(1020) \rightarrow \gamma f_0(980)$  was motivated by the fact that in its framework we can take account of not only the additive quark model processes (emission of the photon by constituent quark) but also those beyond it within the use of the dipole formula (the photon emission by the charge-exchange current gives such an example). The dipole formula for the radiative transition of vector state to scalar one,  $V \rightarrow \gamma S$  was applied before for the calculation of reactions with heavy quarks, see [9, 10] and references therein. Still, a straightforward application of the dipole formula to the reaction  $\phi(1020) \rightarrow \gamma f_0(980)$  is hardly possible, for the  $f_0(980)$  for sure

cannot be represented as a stable particle: this resonance is characterized by two poles laying on two different sheets of the complex- $M$  plane, at  $M = 1020 - i40$  MeV and  $M = 960 - i200$  MeV. It should be emphasized that these two poles are important for the description of  $f_0(980)$ . Therefore we use below the method as follows: we calculate the radiative transition to a stable bare  $f_0$  state (this is  $f_0^{bare}(700 \pm 100)$ , its parameters were obtained in the  $K$ -matrix analysis [1]. In this way we find out the description of the process  $\phi(1020) \rightarrow \gamma f_0^{bare}(700 \pm 100)$  and furthermore we switch on the hadronic decays and determine the transition  $\phi(1020) \rightarrow \gamma\pi\pi$ ; just the residue in the pole of this amplitude is the radiative transition amplitude  $\phi(1020) \rightarrow \gamma f_0(980)$ . Hence we obtain a successful description of data for  $\phi(1020) \rightarrow \gamma\pi\pi$  and  $\phi(1020) \rightarrow \gamma f_0(980)$  within the assumption that  $f_0(980)$  is dominated by the quark-antiquark state.

The conclusion about the nature of  $f_0(980)$  cannot be based on the study of one reaction only but should be motivated by the whole aggregate of data. In the article, we list also the other processes, which provide us with arguments in favour of the dominant  $q\bar{q}$  structure of  $f_0(980)$ .

Section 2 is introductory: here we consider a simple model for the description of composite vector ( $V$ ) and scalar ( $S$ ) particles, the composite particles consisting of one-flavour quark, charge-exchange currents being absent. In such a model the decay transition  $V \rightarrow \gamma S$  is completely determined by the additive quark model process: the photon is emitted only by one or another constituent quark. Two alternative representations of the  $V \rightarrow \gamma S$  decay amplitude are given, namely, the standard additive quark model formula and that of a photon dipole emission, in the latter the factor  $\omega = (m_V - m_S)$  is written in the explicit form. The comparison of these two representations helps us to formulate the problem of application of the threshold theorem [11] to the reaction  $V \rightarrow \gamma S$ . Using a simple example with exponential wave functions, we demonstrate the  $\omega^3$  factor occurred in the partial decay width when the transition  $V \rightarrow \gamma S$  is considered in terms of the additive quark model.

The threshold theorem has a straightforward formulation for the stable  $V$  and  $S$  states but it is not the case for resonances, which are the main objects of our present study. That is why we intend to re-formulate the threshold theorem as the requirement of the amplitude analyticity – this is given in Section 3, on the basis of [12]. Working with non-stable particles, when  $V$  and  $S$  are resonances, the  $V \rightarrow \gamma S$  amplitude should be determined as a residue of a more general amplitude, with stable particles in the initial and final states. For example, the  $\phi(1020) \rightarrow \gamma f_0(980)$  amplitude should be defined as a residue of the  $e^+e^- \rightarrow \gamma\pi\pi$  amplitude in the poles corresponding to resonances  $\phi(1020)$  and  $f_0(980)$  (the  $\phi$  pole in the  $e^+e^-$ -channel and the  $f_0$  pole in the  $\pi\pi$  channel). The only residue in the pole defines the universal amplitude which does not depend on the considered reaction.

In Section 4 we discuss the reaction  $\phi \rightarrow \gamma f_0$  for the case, when the  $f_0$  is a multicomponent system and  $f_0$  and  $\phi$  are stable states with respect to hadronic decays. The analysis of meson spectra (e.g. see the latest  $K$ -matrix analyses [1, 5]) definitely tells us that the  $f_0$ -mesons are the mixture of the quarkonium ( $n\bar{n} = (u\bar{u} + d\bar{d})/\sqrt{2}$  and  $s\bar{s}$ ) and gluonium components. Such a multichannel structure of  $f_0$  states reveals itself in the existence of the  $t$ -channel charge-exchange currents. Therefore, the transition  $\phi \rightarrow \gamma f_0$  goes via two mechanisms: the photon emission by constituent quarks (additive quark model process) and charge-exchange current. We write down

the formulae for the amplitudes initiated by these two mechanisms. The equality to zero of the whole amplitude at small mass difference of  $\phi$  and  $f_0$ ,  $A_{\phi \rightarrow \gamma f_0} \sim \omega$  at  $\omega \rightarrow 0$ , is resulted from the cancellation of contributions of these two mechanisms. We also give a dipole representation of the transition amplitude, where  $A_{\phi \rightarrow \gamma f_0}$  is determined through the mean transition radius and mass difference ( $m_\phi - m_{f_0}$ ).

Section 5 is devoted to the reaction  $\phi(1020) \rightarrow \gamma f_0(980)$ . First, we discuss whether it is possible to treat  $f_0(980)$  as a stable particle. Our answer is "no": in fact the  $f_0(980)$  is unstable particle characterized by two poles located near the  $K\bar{K}$  threshold. As was stressed above, strong transitions  $f_0(980) \rightarrow \pi\pi$ ,  $K\bar{K}$  reveal themselves in the two amplitude poles, which are located on different sheets of the complex  $M$ -plane, at  $M = 1020 - i 40$  MeV and  $M = 960 - i 200$  MeV, and these two poles are important for the description of  $f_0(980)$ . The essential role of the second pole is seen by considering the  $\pi\pi$  spectrum in  $\phi(1020) \rightarrow \gamma\pi\pi$  (Section 6): the visible width of the pick in the  $\pi\pi$  spectrum is of the order of 150 MeV, and the spectrum decreases slowly with further decrease of  $M_{\pi\pi}$ .

Another problem to be discussed is the choice of a method for the consideration of radiative decay amplitude. One can work within two alternative representations for the  $A_{\phi \rightarrow \gamma f_0}$  amplitude. One representation uses additive quark model complemented with the contribution from the charge-exchange current processes. Whence the additive quark model amplitude can be calculated rather definitely, at least for the lowest  $q\bar{q}$  states, the charge-exchange current processes are vaguely determined.

The other way to deal with the transition amplitude consists in using the dipole emission formulae, where the amplitude is defined by the mean transition radius and factor ( $m_\phi - m_{f_0}$ ). For the lowest  $q\bar{q}$  states, we have a good estimate of the radius. But there is a problem of the determination of the factor ( $m_\phi - m_{f_0}$ ), because the  $f_0(980)$  is unstable particle characterized by two poles. The pole  $M = 960 - i 200$  MeV is disposed on the same sheet of the complex- $M$  plane as the pole of  $\phi$ -meson, and the distance  $|m_\phi - m_{f_0}|$  is  $\sim 200$  MeV, while the pole  $M = 1020 - i 40$  MeV is located on another sheet, the distance from the  $\phi$  meson is  $\sim 70$  MeV, that is also not small in the hadronic scale. The problem is what the mass difference factor means in case of complex masses and which pole should be used to characterise this mass difference.

To succeed in the description of the decay  $\phi(1020) \rightarrow \gamma f_0(980)$  we use the results of the  $K$ -matrix analysis of the ( $IJ^{PC} = 00^{++}$ )-wave [1]. The fact is that, on the one hand, the  $K$ -matrix analysis allows us to get the experimentally based information on masses and full widths of resonances together with the pole residues needed for the decay couplings and partial widths. On the other hand, the knowledge of the  $K$ -matrix amplitude enables us to trace the evolution of states by switching on/off the decay channels. In such a way, one may obtain the characteristics of the bare states, which are predecessors of real resonances. With such characteristics, one can perform a reverse procedure: to retrace the transformation of the amplitude written in terms of bare states to the amplitude corresponding to the transition to real resonance. Just this procedure has been applied in Section 5 for the calculation of the decay amplitude  $\phi(1020) \rightarrow \gamma f_0(980)$ .

Therefore, within the frame of non-relativistic quark model, we have calculated the reaction

$\phi(1020) \rightarrow \gamma f_0^{bare}(n)$ , where  $f_0^{bare}(n)$  are bare states found in [1]. Furthermore, with the  $K$ -matrix technique, we have taken account of the decays  $f_0^{bare}(n) \rightarrow \pi\pi, KK$ , thus having calculated the reaction  $\phi(1020) \rightarrow \gamma\pi\pi$  and the amplitude of  $\phi(1020) \rightarrow \gamma f_0(980)$  (the pole residue in the  $\pi\pi$  channel). In this way we see that the main contribution is given by the transition  $\phi(1020) \rightarrow \gamma f_0^{bare}(700 \pm 100)$ . The characteristics of  $f_0^{bare}(700 \pm 100)$  are fixed by the  $K$ -matrix analysis [1]: this is a  $q\bar{q}$  state close to the flavour octet and it is just the predecessor of  $f_0(980)$ . In the framework of this approach we succeed in the description of data for the reactions  $\phi(1020) \rightarrow \gamma f_0(980)$  (Section 5) and  $\phi(1020) \rightarrow \gamma\pi\pi$  (Section 6).

Let us note that such a method, the use of bare states for the calculation of meson spectra, has been applied before for the study weak hadronic decays  $D^+ \rightarrow \pi^+\pi^+\pi^-$  [13] and description of the  $\pi\pi$  spectra in photon–photon collisions  $\gamma\gamma \rightarrow \pi\pi$  [14].

The question of what is the accuracy of the additive quark model in the description of the reactions  $\phi(1020) \rightarrow \gamma f_0^{bare}(700 \pm 100)$  and  $\phi(1020) \rightarrow \gamma f_0(980)$  is discussed in Section 7. We compare the results of the calculation of the  $\phi(1020) \rightarrow \gamma f_0^{bare}(700 \pm 100)$  reaction by using the dipole formula with that of the additive quark model. It is seen that, within error-bars given by the  $K$ -matrix analysis [1], the results coincide. Still, one should emphasize that the dipole-calculation accuracy is low that is due to a large error in the determination of the bare-state masses. The coincidence of results in the dipole and additive quark model formulae should point to a small contribution of processes which violate additivity such as photon emission by the charge-exchange current: this smallness is natural, provided the hadrons are characterized by two sizes, namely, the hadron radius ( $R_h \sim R_{confinement}$ ) and constituent-quark radius ( $r_q$ ) under the condition  $r_q^2 \ll R_h^2$ , see [15] and references therein.

The performed analysis demonstrates that the studied reaction,  $\phi(1020) \rightarrow \gamma f_0(980)$  does not provide us any difficulty with the interpretation of  $f_0(980)$  as  $q\bar{q}$ -state. Still, to conclude about the content of  $f(980)$  we list in Section 8 the arguments in favour of the  $q\bar{q}$  origin of  $f_0(980)$ .

## 2 The process $V \rightarrow \gamma S$ within non-relativistic additive quark model

Here, in the framework of non-relativistic quark model, we consider the transition  $V \rightarrow \gamma S$  in case when the charge-current exchange forces are absent and the  $V \rightarrow \gamma S$  amplitude is given by the additive quark model contribution.

### 2.1 Wave functions for vector and scalar composite particles

The  $q\bar{q}$  wave functions of vector ( $V$ ) and scalar ( $S$ ) particles are defined as follows:

$$\begin{aligned}\Psi_{V\mu}(\mathbf{k}) &= \sigma_\mu \psi_V(k^2) , \\ \Psi_S(\mathbf{k}) &= (\boldsymbol{\sigma} \mathbf{k}) \psi_S(k^2) ,\end{aligned}\tag{1}$$

where, by using Pauli matrices, the spin factors are singled out. The blocks dependent on the relative momentum squared are related to the vertices in the following way:

$$\begin{aligned}\psi_V(k^2) &= \frac{\sqrt{m}}{2} \frac{G_V(k^2)}{k^2 + m\varepsilon_V}, \\ \psi_S(k^2) &= \frac{1}{2\sqrt{m}} \frac{G_S(k^2)}{k^2 + m\varepsilon_V}.\end{aligned}\quad (2)$$

Here  $m$  is the quark mass,  $\varepsilon$  is the composite-system binding energy:  $\varepsilon_V = 2m - m_V$  and  $\varepsilon_S = 2m - m_S$ , where  $m_V$  and  $m_S$  are the masses of bound states. The normalization condition for the wave functions reads:

$$\begin{aligned}\int \frac{d^3k}{(2\pi)^3} \text{Sp}_2 [\Psi_S^+(\mathbf{k}) \Psi_S(\mathbf{k})] &= \int \frac{d^3k}{(2\pi)^3} \psi_S^2(k^2) \text{Sp}_2[(\sigma\mathbf{k})(\sigma\mathbf{k})] = 1, \\ \int \frac{d^3k}{(2\pi)^3} \text{Sp}_2 [\Psi_{V\mu}^+(\mathbf{k}) \Psi_{V\mu'}(\mathbf{k})] &= \int \frac{d^3k}{(2\pi)^3} \psi_V^2(k^2) \text{Sp}_2[\sigma_\mu \sigma_{\mu'}] = \delta_{\mu\mu'}.\end{aligned}\quad (3)$$

## 2.2 Amplitude within additive quark model

When a photon is emitted by quark or antiquark, the  $V \rightarrow \gamma S$  process is described by the triangle diagram, see Fig. 1a, that is actually the contribution from additive quark model. Relativistic consideration of the triangle diagram is presented in [16, 17], while the discussion of non-relativistic approximation is given in [12, 18] (recall that in [18] corresponding wave functions were determined in another way, namely:  $\psi_V(k^2) = G_V(k^2)(4k^2 + 4m\varepsilon_V)^{-1}$  and  $\psi_S(k^2) = G_S(k^2)(4k^2 + 4m\varepsilon_S)^{-1}$ ).

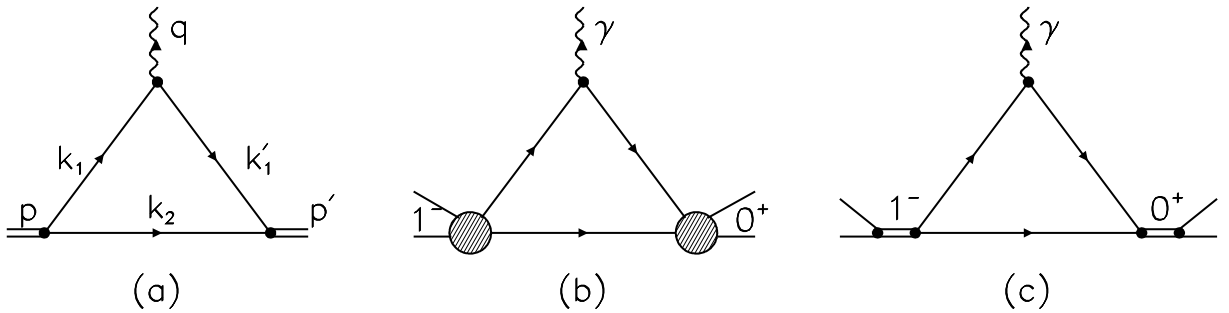


Figure 1: Transitions  $V \rightarrow \gamma S$  in the additive quark model.

In terms of wave functions (1) the triangle-diagram contribution reads:

$$\epsilon_\mu^{(V)} \epsilon_\alpha^{(\gamma)} A_{\mu\alpha}^{V \rightarrow \gamma S} = e Z_{V \rightarrow \gamma S} \epsilon_\mu^{(V)} \epsilon_\alpha^{(\gamma)} F_{\mu\alpha}^{V \rightarrow \gamma S}, \quad (4)$$

$$F_{\mu\alpha}^{V \rightarrow \gamma S} = \int \frac{d^3k}{(2\pi)^3} \text{Sp}_2 [\Psi_S^+(\mathbf{k}) 4k_\alpha \Psi_{V\mu}(\mathbf{k})].$$

Here  $\epsilon_\mu^{(V)}$  and  $\epsilon_\alpha^{(\gamma)}$  are polarization vectors for  $V$  and  $\gamma$ :  $\epsilon_\mu^{(V)} p_{V\mu} = 0$  and  $\epsilon_\alpha^{(\gamma)} q_\alpha = 0$ . The charge factor  $Z_{V \rightarrow \gamma S}$  being different for different reactions is specified below (see also [16, 17]). The expression for the transition amplitude (4) can be simplified after the substitution in the integrand

$$\text{Sp}_2[\sigma_\mu(\sigma \mathbf{k})] k_\alpha \rightarrow \frac{2}{3} k^2 g_{\mu\alpha}^{\perp\perp}, \quad (5)$$

where  $g_{\mu\alpha}^{\perp\perp}$  is the metric tensor in the space orthogonal to total momentum of the vector particle  $p_V$  and photon  $q$ . The substitution (5) results in:

$$A_{\mu\alpha}^{V \rightarrow \gamma S} = e g_{\mu\alpha}^{\perp\perp} A_{V \rightarrow \gamma S}, \quad (6)$$

where

$$A_{V \rightarrow \gamma S} = Z_{V \rightarrow \gamma S} \int_0^\infty \frac{dk^2}{\pi} \psi_S(k^2) \psi_V(k^2) \frac{2}{3\pi} k^3. \quad (7)$$

The amplitudes  $A_{\mu\alpha}^{V \rightarrow \gamma S}$  and  $A_{V \rightarrow \gamma S}$  were used in [16, 17] for the decay amplitude  $\phi(1020) \rightarrow \gamma f_0(980)$  within relativistic treatment of the quark transitions.

However, for our purpose it would be suitable not to deal with Eq. (7) but use the form factor  $F_{\mu\alpha}^{V \rightarrow \gamma S}$  of Eq. (4) re-written in the coordinate representation. One has:

$$\begin{aligned} \Psi_{V\mu}(\mathbf{k}) &= \int d^3r e^{i\mathbf{kr}} \Psi_{V\mu}(\mathbf{r}), \\ \Psi_S(\mathbf{k}) &= \int d^3r e^{i\mathbf{kr}} \Psi_S(\mathbf{r}). \end{aligned} \quad (8)$$

Then the form factor  $F_{\mu\alpha}^{V \rightarrow \gamma S}$  can be represented as follows:

$$F_{\mu\alpha}^{V \rightarrow \gamma S} = \int d^3r \text{Sp}_2 [\Psi_S^+(\mathbf{r}) 4k_\alpha \Psi_{V\mu}(\mathbf{r})], \quad (9)$$

where  $k_\alpha$  is the operator:  $k_\alpha = -i\nabla_\alpha$ . This operator can be written as the commutator of  $r_\alpha$  and  $-\nabla^2/m = T$  (kinetic energy):

$$2im(Tr_\alpha - r_\alpha T) = 4(-i\nabla_\alpha). \quad (10)$$

Let us consider the case when the quark-quark interaction is rather simple, say, it depends on the relative interquark distance with the potential  $U(r)$ . For vector and scalar composite systems we also use additional simplifying assumption: vector and scalar mesons consist of quarks of the same flavour ( $q\bar{q}$ ). Then we have the following Hamiltonian:

$$H = -\frac{\nabla^2}{m} + U(r), \quad (11)$$

and can re-write (10) as

$$2im(Hr_\alpha - r_\alpha H) = 4(-i\nabla_\alpha). \quad (12)$$

After substituting the commutator in (9), the transition form factor for the reaction  $V \rightarrow \gamma S$  reads:

$$F_{\mu\alpha}^{V \rightarrow \gamma S} = \int d^3r \text{Sp}_2 [\Psi_S^+(r) r_\alpha \Psi_{V\mu}(r)] 2im(\varepsilon_V - \varepsilon_S). \quad (13)$$

Here we have used that  $(H + \varepsilon_V)\Psi_V = 0$  and  $(H + \varepsilon_S)\Psi_S = 0$ .

The factor  $(\varepsilon_V - \varepsilon_S)$  in the right-hand side (13) is a manifestation of the threshold theorem: at  $(\varepsilon_V - \varepsilon_S) = (m_S - m_V) \rightarrow 0$  the form factor  $F_{\mu\alpha}^{V \rightarrow \gamma S}$  turns to zero. Actually, in the additive quark model the amplitude of the  $V \rightarrow \gamma S$  transition, being determined by the process of Fig. 1a, cannot be zero if  $V$  and  $S$  are basic states with radial quantum number  $n = 1$ : in this case the wave functions  $\psi_V(k^2)$  and  $\psi_S(k^2)$  do not change sign, and the right-hand side (7) does not equal zero. In order to clarify this point let us consider as an example the exponential approximation for the wave functions  $\psi_V(k^2)$  and  $\psi_S(k^2)$ .

### 2.3 Basic vector and scalar $q\bar{q}$ states: the example of exponential approach to wave functions

We parametrize the ground-state wave functions of scalar and vector particles as follows:

$$\begin{aligned}\Psi_{V_\mu}(r) &= \sigma_\mu \psi_V(r^2), & \psi_V(r^2) &= \frac{1}{2^{5/4} \pi^{3/4} b_V^{3/4}} \exp\left[-\frac{r^2}{4b_V}\right], \\ \Psi_S(r) &= (\boldsymbol{\sigma} \cdot \mathbf{r}) \psi_S(r^2), & \psi_S(r^2) &= \frac{i}{\sqrt{3} 2^{5/4} \pi^{3/4} b_S^{5/4}} \exp\left[-\frac{r^2}{4b_S}\right].\end{aligned}\tag{14}$$

The wave functions with  $n = 1$  have no nodes; numerical factors take account of the normalization conditions:

$$\int d^3r \operatorname{Sp}_2 [\Psi_S^+(r) \Psi_S(r)] = 1, \quad \int d^3r \operatorname{Sp}_2 [\Psi_{V_\mu}^+(r) \Psi_{V_\mu}(r)] = \delta_{\mu\mu'}. \tag{15}$$

With exponential wave functions, the matrix element for  $V \rightarrow \gamma S$  given by the additive quark model diagram, Eq. (9), is equal to

$$\epsilon_\mu^{(V)} \epsilon_\alpha^{(\gamma)} F_{\mu\alpha}^{V \rightarrow \gamma S}(\text{additive}) = (\epsilon^{(V)} \epsilon^{(\gamma)}) \frac{2^{7/2}}{\sqrt{3}} \frac{b_V^{3/4} b_S^{5/4}}{(b_V + b_S)^{5/2}}. \tag{16}$$

Formula for  $F_{\mu\alpha}^{V \rightarrow \gamma S}$  written in the frame of the dipole emission, Eq. (13), reads:

$$\epsilon_\mu^{(V)} \epsilon_\alpha^{(\gamma)} F_{\mu\alpha}^{V \rightarrow \gamma S}(\text{dipole}) = (\epsilon^{(V)} \epsilon^{(\gamma)}) \frac{2^{7/2}}{\sqrt{3}} \frac{b_V^{7/4} b_S^{5/4}}{(b_V + b_S)^{5/2}} m(m_V - m_S). \tag{17}$$

In case under consideration (one-flavour quarks with Hamiltonian given by Eq. (11)), the equations (16) and (17) coincide,  $F_{\mu\alpha}^{V \rightarrow \gamma S}(\text{additive}) = F_{\mu\alpha}^{V \rightarrow \gamma S}(\text{dipole})$ , therefore

$$m(m_V - m_S) = b_V^{-1}, \tag{18}$$

that means that the factor  $(\varepsilon_S - \varepsilon_V)$  in the right-hand side (13) relates to the difference between the  $V$  and  $S$  levels and is defined by  $b_V$  only. In this way, the form factor  $F_{\mu\alpha}^{V \rightarrow \gamma S}$  turns to zero only when  $b_V$  (or  $b_S$ ) tends to the infinity.

The considered example does not mean that the threshold theorem for the reaction  $V \rightarrow \gamma S$  does not work — this tells us only that we should interpret and use it carefully. In the next Section, we discuss how to formulate the threshold theorem based on the requirement of amplitude analyticity, thus getting more information on the threshold theorem applicability.

### 3 Analyticity of the amplitude and the threshold theorem

The threshold theorem can be formulated as the requirement of analyticity of the amplitude. To clarify this statement we consider here not only the transition of the bound states but more general process shown in Fig. 1b, where the interacting constituents being in the vector  $J^P = 1^-$  state emit the photon and then turn into the scalar  $J^P = 0^+$  state. This amplitude has as a subprocess the bound state transition. Namely, the blocks for the rescattering of constituents in Fig. 1b contain the poles related to bound states, see Fig. 1c, and the residues in these poles determine the bound-state transition amplitude (triangle diagram shown as intermediate block in Fig. 1c).

With the notations for invariant mass squares in the initial and final states of Fig. 1b as follows

$$P_V^2 = s_V, \quad P_S^2 = s_S, \quad (19)$$

we can write the spin structures for this more general transition  $V \rightarrow \gamma S$ . The standard representation of this amplitude is:

$$A_{\mu\alpha}^{(V \rightarrow \gamma S)}(s_V, s_S, q^2 \rightarrow 0) = \left( g_{\mu\alpha} - \frac{2q_\mu P_{V\alpha}}{s_V - s_S} \right) A_{V \rightarrow \gamma S}(s_V, s_S, 0). \quad (20)$$

Here we stress that the amplitude  $A_{V \rightarrow \gamma S}$  describes the emission of real photon,  $q^2 = 0$ . In (20), it was taken into account that  $(P_V q) = (s_V - s_S)/2$ . The requirement of analyticity, i.e. the absence of a pole at  $s_V = s_S$ , leads to the condition:

$$\left[ A_{V \rightarrow \gamma S}(s_V, s_S, 0) \right]_{s_V \rightarrow s_S} \rightarrow 0, \quad (21)$$

that is the threshold theorem for the transition amplitude  $V \rightarrow \gamma S$ .

It should be now emphasized that the form of the spin factor in Eq. (20) is not unique. Alternatively, one can write the spin factor as the metric tensor  $g_{\mu\alpha}^{\perp\perp}$  working in the space orthogonal to  $P_V$  and  $q$ , i.e.  $P_{V\mu} g_{\mu\alpha}^{\perp\perp} = 0$  and  $g_{\mu\alpha}^{\perp\perp} q_\alpha = 0$ , see Eq. (5). This metric tensor reads:

$$g_{\mu\alpha}^{\perp\perp}(0) = g_{\mu\alpha} + \frac{4s_V}{(s_V - s_S)^2} q_\mu q_\alpha - \frac{2}{s_V - s_S} (P_{V\mu} q_\alpha + q_\mu P_{V\alpha}), \quad (22)$$

and we have used it in Eq. (6). The uncertainty in the choice of spin factor is due to the fact that the difference

$$g_{\mu\alpha}^{\perp\perp}(0) - \left( g_{\mu\alpha} - \frac{2q_\mu P_{V\alpha}}{s_V - s_S} \right) = 4L_{\mu\alpha}(0), \quad (23)$$

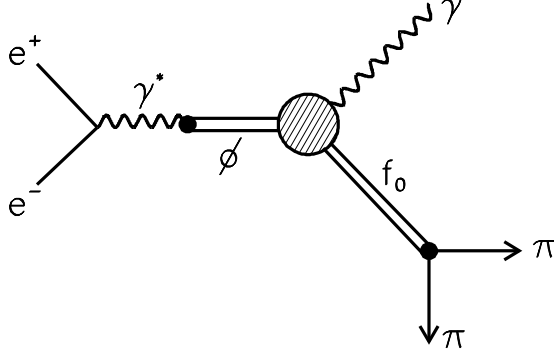


Figure 2: Process  $e^+e^- \rightarrow \gamma\pi\pi$ : residues in the  $e^+e^-$  and  $\pi\pi$  channels determine the  $\phi \rightarrow \gamma f_0$  amplitude.

where

$$L_{\mu\alpha}(0) = \frac{s_V}{(s_V - s_S)^2} q_\mu q_\alpha - \frac{1}{2(s_V - s_S)} P_{V\mu} q_\alpha , \quad (24)$$

is the nilpotent operator [12]:

$$L_{\mu\alpha}(0)L_{\mu\alpha}(0) = 0 . \quad (25)$$

The addition of the nilpotent operator  $L_{\mu\alpha}(0)$  to spin factor of the transition amplitude  $V \rightarrow \gamma S$  does not change the expression  $A_{V \rightarrow \gamma S}(s_V, s_S, 0)$ , see [12] for more detail. Here, by discussing the analytical structure of the amplitude, it is convenient to work with the operator (20), for it is the least cumbersome.

Consider now the reaction  $V \rightarrow \gamma S$  ( $V$  and  $S$  being quark-antiquark bound states), say, of the type of  $\phi \rightarrow \gamma f_0$  or  $\phi \rightarrow \gamma a_0$ . Because of the confinement the quarks are not the particles which form the  $|in\rangle$  and  $\langle out|$  states, therefore the amplitudes like  $A_{\phi \rightarrow \gamma f_0}$  are to be defined as the amplitude residue for the process with the scattering of the stable particles, for example, for  $e^+e^- \rightarrow \gamma\pi^+\pi^-$ , see Fig. 2:

$$A_{\mu\alpha}^{(e^+e^- \rightarrow \gamma\pi^+\pi^-)}(s_V, s_S, 0) = \left( g_{\mu\alpha} - \frac{2q_\mu P_{V\alpha}}{s_V - s_S} \right) \times \\ \times \left[ G_{e^+e^- \rightarrow \phi} \frac{A_{\phi \rightarrow \gamma f_0}(m_\phi^2, m_{f_0}^2, 0)}{(s_V - m_\phi^2)(s_S - m_{f_0}^2)} g_{f_0 \rightarrow \pi^+\pi^-} + B(s_V, s_S, 0) \right] . \quad (26)$$

We see that  $A(m_\phi^2, m_{f_0}^2, 0)$ , up to the factors  $G_{e^+e^- \rightarrow \phi}$  and  $g_{f_0 \rightarrow \pi^+\pi^-}$ , is the residue in the amplitude poles  $s_V = m_\phi^2$  and  $s_S = m_{f_0}^2$ : just this value supplies us with the transition amplitude for the reactions with bound states  $\phi \rightarrow \gamma f_0$ . If we deal with stable composite particles, in other words, if  $\phi$  and  $f_0$  can be included into the set of fields  $|in\rangle$  and  $\langle out|$ , the transition amplitude  $\phi \rightarrow \gamma f_0$  can be written in the form similar to (20):

$$A_{\mu\alpha}^{(\phi \rightarrow \gamma f_0)}(m_\phi^2, m_{f_0}^2, 0) = \left( g_{\mu\alpha} - \frac{2q_\mu p_\alpha}{m_\phi^2 - m_{f_0}^2} \right) A_{\phi \rightarrow \gamma f_0}(m_\phi^2, m_{f_0}^2, 0) , \quad (27)$$

where we have substituted  $P_V \rightarrow p$ . For  $A_{\phi \rightarrow \gamma f_0}(m_\phi^2, m_{f_0}^2, 0)$  the threshold theorem is fulfilled:

$$\left[ A_{\phi \rightarrow \gamma f_0}(m_\phi^2, m_{f_0}^2, 0) \right]_{m_\phi^2 \rightarrow m_{f_0}^2} \sim (m_\phi^2 - m_{f_0}^2) , \quad (28)$$

that means that the threshold theorem of Eq. (28) reveals itself as a requirement of analyticity of the amplitude  $\phi \rightarrow \gamma f_0$  determined by Eq. (27).

Let us emphasize again that formula (27) has been written for the  $\phi$  and  $f_0$  mesons assuming them to be stable, i.e. they can be treated as the states which belong to the sets  $|in\rangle$  and  $\langle out|$ . However, by considering the process  $\phi \rightarrow \gamma f_0$ , we deal with resonances, not stable particles, and whether this assumption is valid for resonances is a question which deserves special discussion. We shall come back to this point below, and so far let us investigate how the requirement (28) is realized in quantum mechanics, when  $\phi$  and  $f_0$  are stable particles.

## 4 Quantum mechanics consideration of the reaction $\phi \rightarrow \gamma f_0$ with $\phi$ and $f_0$ being stable particles

In Section 2, we have considered the model for the reaction  $V \rightarrow \gamma S$ , when  $V$  and  $S$  are formed by quarks of the same flavour (one-channel model for  $V$  and  $S$ ). The one-channel approach for  $\phi(1020)$  (the dominance of  $s\bar{s}$  component) looks acceptable, though for  $f_0$ -mesons it is definitely not so: scalar-isoscalar states are the multicomponent ones.

The existence of several components in the  $f_0$ -mesons changes the situation with the  $\phi \rightarrow \gamma f_0$  decays. First, the mixing of different components may result in close values of masses of the low-lying vector and scalar mesons. Second, equations (9) and (13) for the  $\phi \rightarrow \gamma f_0$  decay turn to be non-equivalent because of the photon emission by the  $t$ -channel exchange currents.

Here we consider in detail a simple model for  $\phi$  and  $f_0$ : the  $\phi$ -meson is treated as  $s\bar{s}$ -system, with no admixture of the non-strange quarkonium,  $n\bar{n} = (u\bar{u} + d\bar{d})/\sqrt{2}$ , nor gluonium ( $gg$ ), while the  $f_0$ -meson is a mixture of  $s\bar{s}$  and  $gg$ .

This model can be considered as a guide for the study of the reaction  $\phi(1020) \rightarrow \gamma f_0(980)$ . Indeed, the  $\phi(1020)$  is almost pure  $s\bar{s}$ -state, the admixture of the  $n\bar{n}$  component in  $\phi(1020)$  is small,  $\leq 5\%$ , and it can be neglected in a rough estimate of the  $\phi(1020) \rightarrow \gamma f_0(980)$  decay.

The resonance  $f_0(980)$  is a multicomponent state. Analysis of the ( $IJ^{PC} = 00^{++}$ )-wave in the K-matrix fit to the data for meson spectra  $\pi\pi$ ,  $K\bar{K}$ ,  $\eta\eta$ ,  $\eta\eta'$ ,  $\pi\pi\pi\pi$  gives the following constraints for the  $s\bar{s}$ ,  $n\bar{n}$  and  $gg$  components in  $f_0(980)$  [1, 5]:

$$\begin{aligned} 50\% &\lesssim W_{s\bar{s}}[f_0(980)] < 100\% , \\ 0 &\lesssim W_{n\bar{n}}[f_0(980)] < 50\% , \\ 0 &\lesssim W_{gg}[f_0(980)] < 25\% . \end{aligned} \quad (29)$$

Also, the  $f_0(980)$  may contain a long-range  $K\bar{K}$  component, on the level of  $10 - 20\%$ .

The restrictions (29) permit the variant, when the probability for the  $n\bar{n}$ -component is small, and  $f_0(980)$  is a mixture of  $s\bar{s}$  and  $gg$  only. Bearing this variant in mind, we consider such

two-component model for  $\phi$  and  $f_0$  supposing these particles are stable in respect to hadronic decays.

It is not difficult to generalise our consideration for the three-component  $f_0$  state ( $n\bar{n}$ ,  $s\bar{s}$  and  $gg$ ), corresponding formulae are given in this Section too.

#### 4.1 Two-component model ( $s\bar{s}$ , $gg$ ) for $f_0$ and $\phi$

Now let us discuss the model, where  $f_0$  has two components only: strange quarkonium ( $s\bar{s}$  in the  $P$ -wave) and gluonium ( $gg$  in the  $S$ -wave). The spin structure of the  $s\bar{s}$  wave function is written in Section 2: it contains the factor  $(\sigma \mathbf{r})$  in the coordinate representation. For the  $gg$  system we have  $\delta_{ab}$  or, in terms of polarization vectors, the convolution  $(\epsilon_1^{(g)} \epsilon_2^{(g)})$ . Here we consider a simple interaction, when the potential does not depend on spin variables, — in this case one may forget about the vector structure of  $gg$  working as if the gluon component consists of spinless particles. As concern  $\phi$ , it is considered as a pure  $s\bar{s}$  state in the  $S$ -wave, with the wave-function spin factor  $\sim \sigma_\mu$ , see Section 2. So, the wave functions of  $f_0$  and  $\phi$  mesons are written as follows:

$$\begin{aligned}\hat{\Psi}_{f_0}(\mathbf{r}) &= \begin{pmatrix} \Psi_{f_0(s\bar{s})}(\mathbf{r}) \\ \Psi_{f_0(gg)}(r) \end{pmatrix} = \begin{pmatrix} (\sigma \mathbf{r}) \psi_{f_0(s\bar{s})}(r) \\ \psi_{f_0(gg)}(r) \end{pmatrix}, \\ \hat{\Psi}_{\phi\mu}(\mathbf{r}) &= \begin{pmatrix} \Psi_{\phi(s\bar{s})\mu}(\mathbf{r}) \\ \Psi_{\phi(gg)\mu}(r) \end{pmatrix} = \begin{pmatrix} \sigma_\mu \psi_{\phi(s\bar{s})}(r) \\ 0 \end{pmatrix}.\end{aligned}\quad (30)$$

The normalization condition is given by Eq. (15), with the obvious replacement:  $\Psi_S \rightarrow \hat{\Psi}_{f_0}$  and  $\Psi_{V\mu} \rightarrow \hat{\Psi}_{\phi\mu}$ .

The Shrödinger equation for the two-component states,  $s\bar{s}$  and  $gg$ , reads:

$$\begin{vmatrix} \frac{1}{m}k^2 + U_{s\bar{s} \rightarrow s\bar{s}}(r) & U_{s\bar{s} \rightarrow gg}(\mathbf{r}) \\ U_{s\bar{s} \rightarrow gg}^+(\mathbf{r}) & \frac{1}{m_g}k^2 + U_{gg \rightarrow gg}(r) \end{vmatrix} \cdot \begin{pmatrix} \Psi_{s\bar{s}}(\mathbf{r}) \\ \Psi_{gg}(\mathbf{r}) \end{pmatrix} = E \begin{pmatrix} \Psi_{s\bar{s}}(\mathbf{r}) \\ \Psi_{gg}(\mathbf{r}) \end{pmatrix}. \quad (31)$$

Furthermore we denote the Hamiltonian in the left-hand side (31) as  $H_0$ .

We put the  $gg$  component in  $\phi$  to be zero. It means that the potential  $U_{s\bar{s} \rightarrow gg}(\mathbf{r})$  satisfies the following constraints:

$$\langle 0^+ s\bar{s} | U_{s\bar{s} \rightarrow gg}(\mathbf{r}) | 0^+ gg \rangle \neq 0, \quad \langle 1^- s\bar{s} | U_{s\bar{s} \rightarrow gg}(\mathbf{r}) | 1^- gg \rangle = 0. \quad (32)$$

These constraints do not look surprising for mesons in the region  $1.0 - 1.5$  GeV because the scalar glueball is located just in this mass region, while the vector one has considerably higher mass,  $\sim 2.5$  GeV [19].

The  $t$ -exchange diagrams shown in Fig. 3a,b,c are the example of interaction leading to the potentials  $U_{s\bar{s} \rightarrow s\bar{s}}(r)$ ,  $U_{gg \rightarrow gg}(r)$  and  $U_{s\bar{s} \rightarrow gg}(\mathbf{r})$ . The potential  $U_{s\bar{s} \rightarrow gg}(\mathbf{r})$  contains the  $t$ -channel charge exchange.

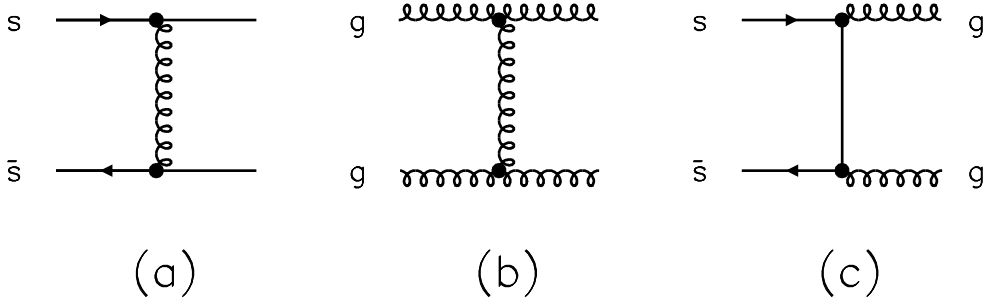


Figure 3: Examples of diagrams, which contribute to the potentials  $U_{s\bar{s} \rightarrow s\bar{s}}(r)$ ,  $U_{s\bar{s} \rightarrow gg}(\mathbf{r})$  and  $U_{gg \rightarrow gg}(r)$ .

#### 4.1.1 Dipole emission of the photon in $\phi \rightarrow \gamma f_0$ decay

The Hamiltonian for the interaction of electromagnetic field with two-component composite systems (quarkonium and gluonium components) is presented in Appendix A.

For the transition  $V \rightarrow \gamma S$ , keeping the terms proportional to the charge  $e$ , we have the following operator for the dipole emission:

$$\hat{d}_\alpha = \begin{vmatrix} 2k_\alpha & , & ir_\alpha U_{s\bar{s} \rightarrow gg}(\mathbf{r}) \\ -ir_\alpha U_{s\bar{s} \rightarrow gg}^+(\mathbf{r}) & , & 0 \end{vmatrix}. \quad (33)$$

The transition form factor is given by the formula similar to Eq. (9) for the one-channel case, it reads:

$$F_{\mu\alpha}^{\phi \rightarrow \gamma f_0} = \int d^3r \text{Sp}_2 [\hat{\Psi}_{f_0}^+(\mathbf{r}) 2\hat{d}_\alpha \hat{\Psi}_{\phi\mu}(\mathbf{r})]. \quad (34)$$

Drawing explicitly the two-component wave functions, one can re-write Eq. (34) as follows:

$$\begin{aligned} F_{\mu\alpha}^{\phi \rightarrow \gamma f_0} &= \int d^3r \text{Sp}_2 [\Psi_{f_0(s\bar{s})}^+(\mathbf{r}) 4k_\alpha \Psi_{\phi(s\bar{s})\mu}(\mathbf{r})] + \\ &+ \int d^3r \text{Sp}_2 [\Psi_{f_0(gg)}^+(\mathbf{r}) (-ir_\alpha U_{gg \rightarrow s\bar{s}}(\mathbf{r})) \Psi_{\phi(s\bar{s})\mu}(\mathbf{r})]. \end{aligned} \quad (35)$$

The first term in the right-hand side (35), with the operator  $4k_\alpha$ , is responsible for the interaction of a photon with constituent quark that is the additive quark model contribution, while the term  $(-ir_\alpha U_{gg \rightarrow s\bar{s}}(\mathbf{r}))$  describes interaction of the photon with the charge flowing through the  $t$ -channel – this term describes the photon interaction with the fermion exchange current.

Let us return to Eq. (34) and re-write it in the form similar to (13). One can see that

$$im (\hat{H}_0 \hat{r}_\alpha - \hat{r}_\alpha \hat{H}_0) = \hat{d}_\alpha, \quad (36)$$

where  $\hat{H}_0$  is the Hamiltonian for composite systems written in the left-hand side (31), and the operator  $\hat{r}_\alpha$  is determined as

$$\hat{r}_\alpha = \begin{pmatrix} r_\alpha & 0 \\ 0 & 0 \end{pmatrix}. \quad (37)$$

Substituting Eq. (36) to (34), we have

$$F_{\mu\alpha}^{\phi \rightarrow \gamma f_0} = \int d^3r \text{Sp}_2 [(\boldsymbol{\sigma} \mathbf{r}) \psi_{f_0(s\bar{s})}(r) r_\alpha \sigma_\mu \psi_{\phi(s\bar{s})}(r)] 2im(\varepsilon_\phi - \varepsilon_{f_0}). \quad (38)$$

This formula for the dipole emission of photon is similar to that of (13) for the one-channel model.

#### 4.1.2 Partial width of the decay $\phi \rightarrow \gamma f_0$

Partial width of the decay  $\phi \rightarrow f_0$  in case, when  $\phi$  is pure  $s\bar{s}$  state, is determined by the following formula:

$$m_\phi \Gamma_{\phi \rightarrow \gamma f_0} = \frac{1}{6} \alpha \frac{m_\phi^2 - m_{f_0}^2}{m_\phi^2} |A_{\phi \rightarrow \gamma f_0(s\bar{s})}|^2 \quad (39)$$

where  $\alpha = 1/137$  and the  $A_{\phi \rightarrow \gamma f_0(s\bar{s})}$  amplitude is determined by Eq. (6) (here it is specified that we deal with  $s\bar{s}$  quarks in the intermediate state).

### 4.2 Three-component model ( $s\bar{s}$ , $n\bar{n}$ , $gg$ ) for $f_0$ and $\phi$

The above formula can be easily generalized for the case, when  $f_0$  is the three-component system ( $s\bar{s}$ ,  $n\bar{n}$ ,  $gg$ ) and  $\phi$  is two-component one ( $s\bar{s}$ ,  $n\bar{n}$ ), while  $gg$  is supposed to be negligibly small. We have two transition form factors:

$$F_{\mu\alpha}^{\phi \rightarrow \gamma f_0(s\bar{s})} = \int d^3r \text{Sp}_2 [(\boldsymbol{\sigma} \mathbf{r}) \psi_{f_0(s\bar{s})}(r) r_\alpha \sigma_\mu \psi_{\phi(s\bar{s})}(r)] 2im(\varepsilon_\phi - \varepsilon_{f_0}), \quad (40)$$

and

$$F_{\mu\alpha}^{\phi \rightarrow \gamma f_0(n\bar{n})} = \int d^3r \text{Sp}_2 [(\boldsymbol{\sigma} \mathbf{r}) \psi_{f_0(n\bar{n})}(r) r_\alpha \sigma_\mu \psi_{\phi(n\bar{n})}(r)] 2im(\varepsilon_\phi - \varepsilon_{f_0}). \quad (41)$$

The partial width reads:

$$m_\phi \Gamma_{\phi \rightarrow \gamma f_0} = \frac{1}{6} \alpha \frac{m_\phi^2 - m_{f_0}^2}{m_\phi^2} |A_{\phi \rightarrow \gamma f_0(s\bar{s})} + A_{\phi \rightarrow \gamma f_0(n\bar{n})}|^2, \quad (42)$$

with  $A_{\phi \rightarrow \gamma f_0}$  defined by Eqs. (4) and (6). The charge factors, which were separated in Eq. (4), are equal to:

$$Z_{\phi \rightarrow \gamma f_0}^{(s\bar{s})} = -\frac{2}{3}, \quad Z_{\phi \rightarrow \gamma f_0}^{(n\bar{n})} = \frac{1}{3}, \quad (43)$$

they include the combinatorics factor 2 related to two diagrams with the photon emmision by quark and antiquark, see [16, 17] for more detail.

## 5 Decay $\phi(1020) \rightarrow \gamma f_0(980)$

The vector meson  $\phi(1020)$  has rather small decay width,  $\Gamma_{\phi(1020)} \simeq 4.5$  MeV; from this point of view there is no doubt that treating  $\phi(1020)$  as stable particle is reasonable. As to  $f_0(980)$ , the picture is not so determinate. In the PDG compilation [20], the  $f_0(980)$  width is given in the interval  $40 \leq \Gamma_{f_0(980)} \leq 100$  MeV, and the width uncertainty is related not to the data unaccuracy (experimental data are rather good) but a vague definition of the width.

The mass and width of the resonance are determined by the pole position in the complex-mass plane,  $M = m - i\Gamma/2$ , — just this magnitude is a universal characteristics of the resonance.

### 5.1 The $f_0(980)$ : position of poles

The definition of the  $f_0(980)$  width is aggravated by the  $K\bar{K}$  threshold singularity that leads to the existence of two, not one, poles. According to the  $K$ -matrix analyses [1, 5], there are two poles in the ( $IJ^{PC} = 00^{++}$ )-wave at  $s \sim 1.0$  GeV<sup>2</sup>,

$$M^I \simeq 1.020 - i0.040 \text{ GeV}, \quad M^{II} \simeq 0.960 - i0.200 \text{ GeV}, \quad (44)$$

which are located on the different complex- $M$  sheets related to the  $K\bar{K}$ -threshold, see Fig. 4. By switching off the decay  $f_0(980) \rightarrow K\bar{K}$ , both poles begin to move to one another, and they coincide after switching off the  $K\bar{K}$  channel completely. Usually, when one discusses the  $f_0(980)$ , the resonance is characterised by the closest pole,  $M^I$ . However, when we are interested in how far from each other the  $\phi(1020)$  and  $f_0(980)$  are, one should not forget about the second pole.

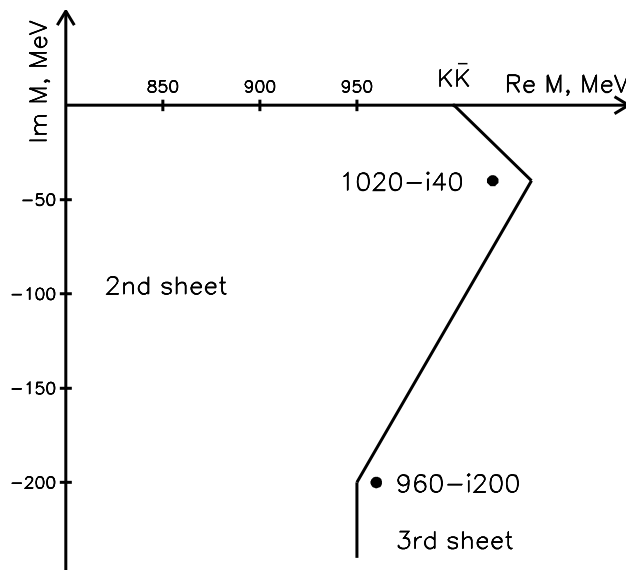


Figure 4: Complex- $M$  plane and location of the poles corresponding to  $f_0(980)$ ; the cut related to the  $K\bar{K}$  threshold is shown as broken line.

Keeping in mind the existence of two poles, one should accept that  $\phi(1020)$  and  $f_0(980)$  are considerably "separated" from each other, and the  $f_0(980)$  resonance can hardly be represented as stable particle – we return to this point once more in Section 6 discussing the  $\pi\pi$  spectrum in  $\phi(1020) \rightarrow \gamma\pi\pi$ .

## 5.2 Switching off decay channels: bare states in $K$ -matrix analysis of the ( $IJ^{PC} = 00^{++}$ )-wave

A significant trait of the  $K$ -matrix analysis is that it also gives us, along with the characteristics of real resonances, the positions of levels before the onset of the decay channels, i.e. it determines the bare states. In addition, the  $K$ -matrix analysis allows one to observe the transform of bare states into real resonances. In Fig. 5, one can see such a transform of the  $00^{++}$ -amplitude poles by switching off the decays  $f_0 \rightarrow \pi\pi, K\bar{K}, \eta\eta, \eta\eta', \pi\pi\pi\pi$ . It is seen that, after switching off the decay channels, the  $f_0(980)$  turns into stable state, approximately 300 MeV lower:

$$f_0(980) \longrightarrow f_0^{\text{bare}}(700 \pm 100) . \quad (45)$$

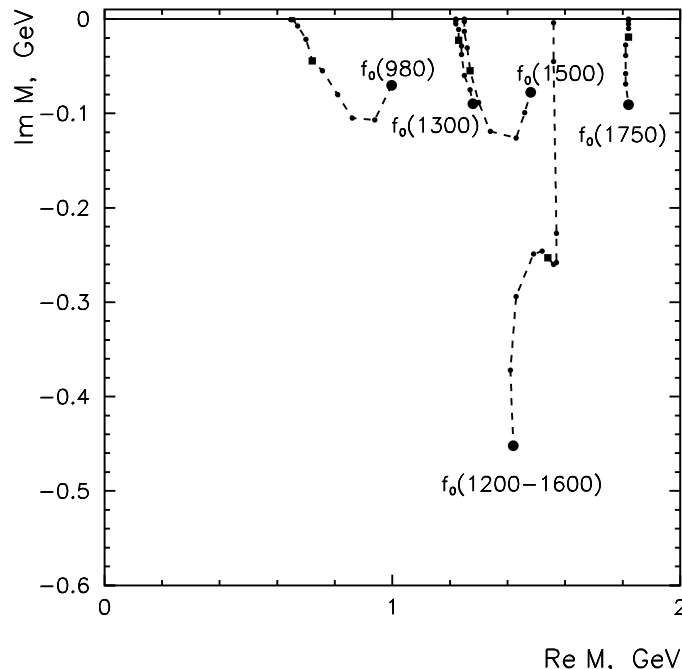


Figure 5: Complex  $M$  plane: trajectories of poles corresponding to the states  $f_0(980)$ ,  $f_0(1300)$ ,  $f_0(1500)$ ,  $f_0(1750)$ ,  $f_0(1200 - 1600)$  within a uniform onset of the decay channels.

The transform of bare states into real resonances can be illustrated by Fig. 6 for the levels in the potential well: bare states are the levels in a well with impenetrable wall (Fig. 6a); at

the onset of the decay channels (under-barrier transitions, Fig. 6b) the stable levels transform into real resonance.

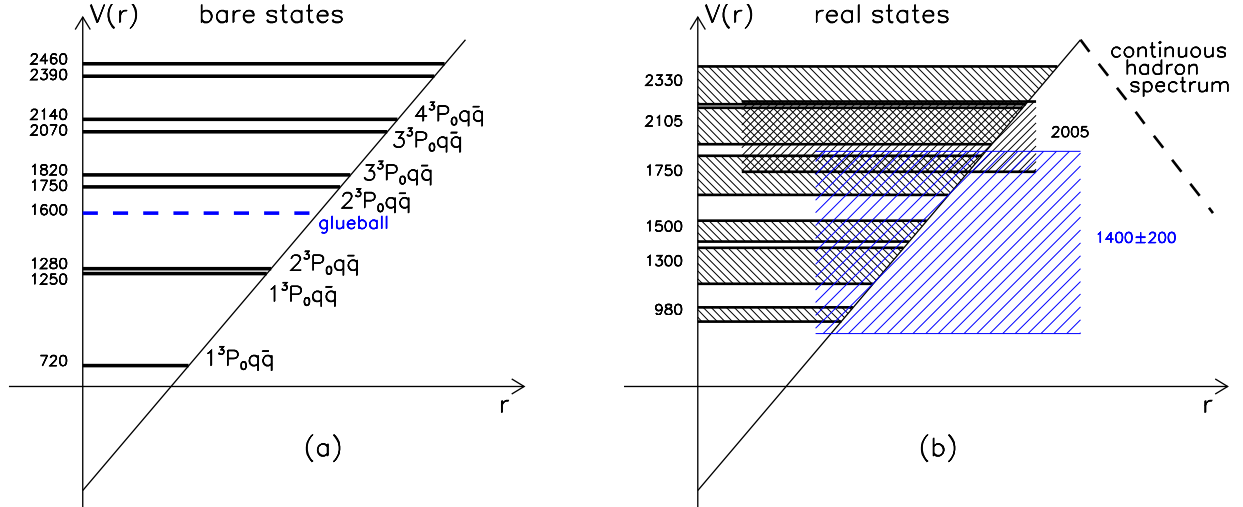


Figure 6: The  $f_0$ -levels in the potential well depending on the onset of the decay channels: bare states (a) and real resonances (b).

Figure 7 demonstrates the evolution of coupling constants at the onset of the decay channels: following [21], relative changes of the coupling constants are shown for  $f_0(980)$  after switching on/off the decay channels. The onset of the decay channels is regulated by the parameter  $x$ , and the value  $x = 0$  corresponds to the bare state (amplitude pole on the  $(\text{Re } M)$ -axis) and the value  $x = 1$  stands for the resonance observed experimentally.

Let us bring the attention to a rapid increase of the coupling constant  $f_0 \rightarrow K\bar{K}$  on the evolution curve  $f_0^{\text{bare}}(700) - f_0(980)$  in the region  $x \sim 0.8 - 1.0$ , where  $\gamma^2(x = 1.0) - \gamma^2(x = 0.8) \simeq 0.2$ , see Fig. 7. Actually this increase allows one to estimate a possible admixture of the long-range  $K\bar{K}$  component in the  $f_0(980)$ : it cannot be greater than 20%.

### 5.3 Calculation of the decay amplitude $\phi(1020) \rightarrow \gamma f_0(980)$

The above discussion of the location of the amplitude poles of  $f_0(980)$  as well as the movement of poles by switching off the decay channels tell us definitely that the smallness of the amplitude of the  $\phi(1020) \rightarrow \gamma f_0(980)$  decay due to a visible proximity of masses of vector and scalar particles is rather questionable. As to  $f_0(980)$ , its poles "dived" into complex plane, in the average in  $\sim 100$  MeV (40 MeV for one pole and 200 MeV for another). But when we intend to represent  $f_0(980)$  as a stable level, one should bear in mind that the mass of the stable level is below the mass of  $\phi(1020)$  in  $\sim 300$  MeV — this value is given by the  $K$ -matrix analysis. In both cases we deal with the shifts in mass scale of the order of pion mass, that is hardly small in hadronic scale.

The  $K$ -matrix amplitude of the  $00^{++}$ -wave reconstructed in [1] gives us the possibility to trace the evolution of the transition form factor  $\phi(1020) \rightarrow \gamma f_0^{\text{bare}}(700 \pm 100)$  during the trans-

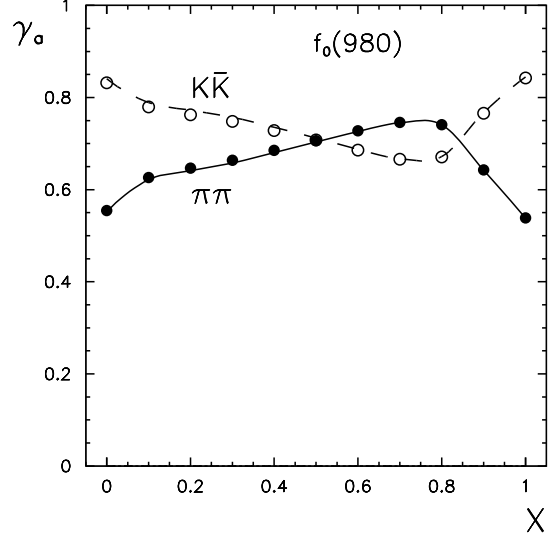


Figure 7: The evolution of normalized coupling constants  $\gamma_a = g_a / \sqrt{\sum_b g_b^2}$  at the onset of the decay channels for  $f_0(980)$ .

formation of the bare state  $f_0^{bare}(700 \pm 100)$  into the  $f_0(980)$  resonance. Using the diagrammatic language, one can say that the evolution of the form factor  $F_{\phi \rightarrow \gamma f_0}^{(bare)}$  is due to the processes shown in Fig. 8:  $\phi$ -meson goes into  $f_0^{bare}(n)$ , with the emission of a photon, then  $f_0^{bare}(n)$  decays into mesons  $f_0^{bare}(n) \rightarrow h_a h_a = \pi\pi, K\bar{K}, \eta\eta, \eta\eta', \pi\pi\pi\pi$ . The decay yields may rescatter thus coming to final states

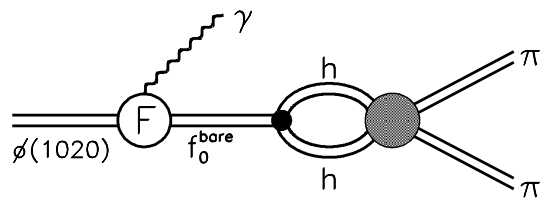


Figure 8: Diagram for the transition  $\phi(1020) \rightarrow \gamma\pi\pi$  in the K-matrix representation, Eq. (46).

The residue of the amplitude pole  $\phi(1020) \rightarrow \gamma\pi\pi$  gives us the transition amplitude  $\phi(1020) \rightarrow \gamma f_0(980)$ . So, in the  $K$ -matrix representation the amplitude of the reaction  $\phi(1020) \rightarrow$

$\gamma\pi\pi$ , Fig. 8, reads:

$$A_{\phi(1020) \rightarrow \gamma\pi\pi}(s) = \sum_{a,n} \frac{F_{\phi(1020) \rightarrow \gamma f_0^{bare}(n)}^{(bare)}}{M_n^2 - s} g_a^{bare}(n) \left( \frac{1}{1 - i\hat{\rho}(s)\hat{K}(s)} \right)_{a,\pi\pi}. \quad (46)$$

Here  $M_n$  is the mass of bare state,  $g_a^{bare}(n)$  is the coupling for the transition  $f_0^{bare}(n) \rightarrow a$ , where  $a = \pi\pi, K\bar{K}, \eta\eta, \eta\eta', \pi\pi\pi\pi$ . The matrix element  $(1 - i\hat{\rho}(s)\hat{K}(s))^{-1}$  takes account of the rescatterings of the formed mesons. Here  $\hat{\rho}(s)$  is the diagonal matrix of phase spaces for hadronic states (for example, for the  $\pi\pi$  system it reads:  $\rho_{\pi\pi}(s) = \sqrt{(s - 4m_\pi^2)/s}$ ), and the  $K$ -matrix elements  $K_{ab}(s)$  contain the poles corresponding to the bare states:

$$K_{ab}(s) = \sum_n \frac{g_a^{bare}(n)g_b^{bare}(n)}{M_n^2 - s} + f_{ab}(s). \quad (47)$$

The function  $f_{ab}(s)$  is analytical in the right-hand half-plane of the complex- $s$  plane, at  $\text{Re } s > 0$ , see [1] for more detail.

Near the pole corresponding to  $f_0$ -resonance (resonance poles are contained in the factor  $(1 - i\hat{\rho}(s)\hat{K}(s))^{-1}$ ), the amplitude  $\phi(1020) \rightarrow \gamma\pi\pi$  is written as follows:

$$A_{\phi(1020) \rightarrow \gamma\pi\pi}(s) \simeq \frac{A_{\phi(1020) \rightarrow \gamma f_0(980)}}{M_{f_0(980)}^2 - s} g_{f_0(980) \rightarrow \pi\pi} + \text{smooth terms} , \quad (48)$$

where  $M_{f_0(980)}$  is the complex-valued resonance mass:  $M_{f_0(980)} \rightarrow M^I \simeq 1.020 - i0.040$  GeV for the first pole, and  $M_{f_0(980)} \rightarrow M^{II} \simeq 0.960 - i0.200$  GeV for the second one. The transition amplitude  $A_{\phi(1020) \rightarrow \gamma f_0(980)}$  is different for different poles; the  $g_{f_0(980) \rightarrow \pi\pi}$  couplings are different as well.

We see that the radiative transition  $\phi(1020) \rightarrow \gamma f_0(980)$  is determined by two amplitudes,  $A_{\phi(1020) \rightarrow \gamma f_0(M^I)} \equiv A_{\phi(1020) \rightarrow \gamma f_0(980)}^I$  and  $A_{\phi(1020) \rightarrow \gamma f_0(M^{II})} \equiv A_{\phi(1020) \rightarrow \gamma f_0(980)}^{II}$ , and just these amplitudes are the subject of our interest. The amplitudes  $A_{\phi(1020) \rightarrow \gamma f_0(980)}^I, A_{\phi(1020) \rightarrow \gamma f_0(980)}^{II}$  may be represented as the sum of contributions from different bare states:

$$A_{\phi(1020) \rightarrow \gamma f_0(980)}^I = \sum_n \zeta_n^I[f_0(980)] F_{\phi(1020) \rightarrow \gamma f_0^{bare}(n)}^{(bare)} , \quad (49)$$

$$A_{\phi(1020) \rightarrow \gamma f_0(980)}^{II} = \sum_n \zeta_n^{II}[f_0(980)] F_{\phi(1020) \rightarrow \gamma f_0^{bare}(n)}^{(bare)} ,$$

To calculate the constants  $\zeta_n[f_0(m_R)]$  we use the  $K$ -matrix solution for the  $00^{++}$ -wave amplitude denoted in [1] as II-2. In this solution, there are five bare states  $f_0^{bare}(n)$  in the mass interval 290–1950 MeV: four of them are members of the  $q\bar{q}$  nonets ( $1^3P_0 q\bar{q}$  and  $2^3P_0 q\bar{q}$ ) and the fifth state is the glueball. Namely:

$$\begin{aligned} 1^3P_0 q\bar{q} : & \quad f_0^{bare}(700 \pm 100), \quad f_0^{bare}(1220 \pm 30), \\ 2^3P_0 q\bar{q} : & \quad f_0^{bare}(1230 \pm 40), \quad f_0^{bare}(1800 \pm 40), \\ \text{glueball} : & \quad f_0^{bare}(1580 \pm 50) . \end{aligned} \quad (50)$$

For the first pole of the  $f_0(980)$ -resonance located at  $M[f_0(980)] = 1020 - i40$  MeV the renormalization constants are as follows:

$$\begin{aligned}\zeta_{700}^{(I)}[f_0(980)] &= 0.62 \exp(-i144^\circ), \\ \zeta_{1220}^{(I)}[f_0(980)] &= 0.37 \exp(-i41^\circ), \\ \zeta_{1230}^{(I)}[f_0(980)] &= 0.19 \exp(i1^\circ), \\ \zeta_{1800}^{(I)}[f_0(980)] &= 0.02 \exp(-i112^\circ), \\ \zeta_{1580}^{(I)}[f_0(980)] &= 0.02 \exp(i5^\circ).\end{aligned}\quad (51)$$

These constants are complex-valued. One should pay attention to the fact that the phases of constants  $\zeta_{700}^{(I)}[f_0(980)]$  and  $\zeta_{1220}^{(I)}[f_0(980)]$  have the relative shift close to  $90^\circ$ . This means that the contributions from  $f_0^{bare}(700 \pm 100)$  and  $f_0^{bare}(1220 \pm 30)$  (which are members of the basic  $1^3P_0 q\bar{q}$  nonet) do not interfere practically in the calculation of probability for the decay  $\phi(1020) \rightarrow \gamma f_0(980)$ .

Actually one may neglect the bare states  $f_0^{bare}(1230)$ ,  $f_0^{bare}(1800)$ ,  $f_0^{bare}(1580)$  in the calculation of the  $\phi(1020) \rightarrow \gamma f_0(980)$  reaction, because the form factors for the production of radial excited states are noticeably suppressed, see [17]:

$$\left| F_{\phi(1020) \rightarrow \gamma f_0(2^3P_0 q\bar{q})}^{(bare)} \right| \ll \left| F_{\phi(1020) \rightarrow \gamma f_0(1^3P_0 q\bar{q})}^{(bare)} \right|.$$

Besides, the coefficients  $\zeta_{1230}^{(I)}[f_0(980)]$ ,  $\zeta_{1800}^{(I)}[f_0(980)]$  are also comparatively small, see (51).

The second pole located on the third sheet,  $M[f_0(980)] = 960 - i200$  MeV, has renormalizing constants as follows:

$$\begin{aligned}\zeta_{700}^{(II)}[f_0(980)] &= 1.00 \exp(i6^\circ), \\ \zeta_{1220}^{(II)}[f_0(980)] &= 0.33 \exp(i113^\circ), \\ \zeta_{1230}^{(II)}[f_0(980)] &= 0.32 \exp(i148^\circ), \\ \zeta_{1800}^{(II)}[f_0(980)] &= 0.08 \exp(i4^\circ), \\ \zeta_{1580}^{(II)}[f_0(980)] &= 0.04 \exp(i98^\circ).\end{aligned}\quad (52)$$

Here, as before, the transitions  $\phi(1020) \rightarrow \gamma f_0^{bare}(1230)$ ,  $\gamma f_0^{bare}(1580)$ ,  $\gamma f_0^{bare}(1800)$  are negligibly small.

In  $\phi(1020)$ , the admixture of the  $n\bar{n}$ -component is small. In the estimates given below we assume  $\phi(1020)$  to be pure  $s\bar{s}$ -state. The bare states  $f_0^{bare}(700)$  and  $f_0^{bare}(1220)$  are mixtures of the  $n\bar{n}$  and  $s\bar{s}$  components

$$n\bar{n} \cos \varphi + s\bar{s} \sin \varphi,$$

and, according to [1], the mixing angles are as follows:

$$\begin{aligned}\varphi \left[ f_0^{bare}(700) \right] &= -70^\circ \pm 10^\circ, \\ \varphi \left[ f_0^{bare}(1220) \right] &= 20^\circ \pm 10^\circ.\end{aligned}\quad (53)$$

Because of that the transition amplitude for  $\phi(1020) \rightarrow \gamma f_0(980)$  reads:

$$\begin{aligned} A_{\phi(1020) \rightarrow \gamma f_0(980)}^N &\simeq \zeta_{700}^N[f_0(980)] \sin \varphi \left[ f_0^{bare}(700) \right] F_{\phi(1020) \rightarrow \gamma f_0^{bare}(700)}^{(bare)} \\ &+ \zeta_{1220}^N[f_0(980)] \sin \varphi \left[ f_0^{bare}(1220) \right] F_{\phi(1020) \rightarrow \gamma f_0^{bare}(1220)}^{(bare)}. \end{aligned} \quad (54)$$

Here  $\zeta_{700}^N[f_0(980)]$  and  $\zeta_{1220}^N[f_0(980)]$  ( $N = I, II$ ) are given by the formulae (51), (52). One can see that numerically the factor  $\zeta_{1220}^N[f_0(980)] \sin \varphi \left[ f_0^{bare}(1220) \right]$  is small, and we may neglect the second term in the right-hand side (54). Then for the pole, which is the closest one to the real axis (1020-i40 MeV), one has:

$$A_{\phi(1020) \rightarrow \gamma f_0(980)}^I \simeq (0.58 \pm 0.04) F_{\phi(1020) \rightarrow \gamma f_0^{bare}(700)}^{(bare)}, \quad (55)$$

and for the distant one, (960-i200 MeV):

$$A_{\phi(1020) \rightarrow \gamma f_0(980)}^{II} \simeq (0.92 \pm 0.06) F_{\phi(1020) \rightarrow \gamma f_0^{bare}(700)}^{(bare)}. \quad (56)$$

We see that practically the  $A_{\phi(1020) \rightarrow \gamma f_0(980)}^{II}$  amplitude does not change its value during the evolution from bare state to resonance, while the decrease of  $A_{\phi(1020) \rightarrow \gamma f_0(980)}^I$  is significant.

## 5.4 Comparison with data

Comparing the above-written formulae with experimental data we have parametrized the wave functions of the  $q\bar{q}$  states in the simplest, exponent-type, form (see Section 2.3). For  $\phi(1020)$ , we accept its mean radius square to be close to the pion radius,  $R_{\phi(1020)}^2 \simeq R_\pi^2$ : both states are members of the same 36-plet. This value of the mean radius square for  $\phi(1020)$  fixes its wave function by  $b_\phi = 10 \text{ GeV}^{-2}$ .

For  $f_0^{bare}(700)$ , we change the value  $b_{f_0}$  in the interval

$$5 \text{ GeV}^{-2} \leq b_{f_0}^{bare} \leq 15 \text{ GeV}^{-2}$$

that corresponds to the interval  $(0.5 \div 1.5)R_\pi^2$  of the mean radius square of  $f_0^{bare}(700)$ .

Using the branching ratios [22, 23] as follows:

$$BR[\phi(1020) \rightarrow \gamma f_0(980)] = (3.5 \pm 0.3_{-0.5}^{+1.3}) \cdot 10^{-4}, \quad (57)$$

$$BR[\phi(1020) \rightarrow \gamma f_0(980)] = (2.90 \pm 0.21 \pm 1.54) \cdot 10^{-4},$$

and the definition of the radiative decay width:

$$m_\phi \Gamma_{\phi \rightarrow \gamma f_0} = \frac{1}{6} \alpha \frac{m_\phi^2 - m_{f_0}^2}{m_\phi^2} |A_{\phi \rightarrow \gamma f_0}|^2,$$

we have the following experimental value for the decay amplitude:

$$A_{\phi(1020) \rightarrow \gamma f_0(980)}^{(exp)} = 0.115 \pm 0.040 \text{ GeV}. \quad (58)$$

Here  $\alpha = 1/137$ ,  $m_\phi = 1.02$  GeV and  $m_{f_0} = 0.975$  GeV (the mass reported in [22, 23] for the measured  $\gamma f_0(980)$  signal) and  $\Gamma_{tot}[\phi(1020)] = 4.26 \pm 0.05$  MeV [20]. The right-hand side (58) should be compared with  $A_{\phi(1020) \rightarrow \gamma f_0(980)}$  calculated with Eqs. (17), (38), and (55):

$$A_{\phi(1020) \rightarrow \gamma f_0(980)}^{(calc)}(\text{dipole}) \simeq (0.58 \pm 0.04) \cdot \sqrt{W_{q\bar{q}}[f_0^{bare}(700)]} Z_{\phi \rightarrow \gamma f_0}^{(s\bar{s})} \cdot$$

$$\cdot \frac{2^{7/2}}{\sqrt{3}} \frac{b_\phi^{7/4} b_{f_0}^{5/4}}{(b_\phi + b_{f_0})^{5/2}} m_s [m_\phi - (0.7 \pm 0.1) \text{GeV}] .$$

Recall, in (59) the factor  $(0.58 \pm 0.04)$  takes into account the change of the transition amplitude caused by the final-state hadron interaction, Eq. (55). The probability to find quark-antiquark component in the bare state  $f_0^{bare}(700)$  is denoted as  $W_{q\bar{q}}[f_0^{bare}(700)]$ : one can guess that it is of the order of 80 – 90%, or even more. The mass of the strange constituent quark is equal to  $m_s \simeq 0.5$  GeV. The wave functions of  $\phi(1020)$  and  $f_0^{bare}(700)$  are parametrized as exponents: we fix  $b_\phi = 10$   $\text{GeV}^{-2}$  (that gives for the mean radius of  $\phi(1020)$  the value of the order of the pion radius,  $R_\phi \simeq R_\pi$ ), and vary  $b_{f_0}$  in the interval  $(5 - 15)$   $\text{GeV}^{-2}$ .

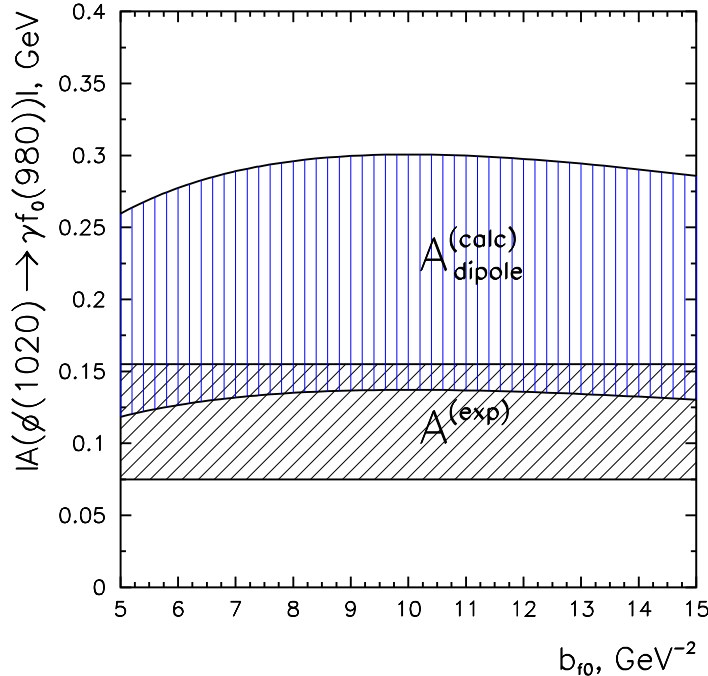


Figure 9: Amplitudes for the decay  $\phi(1020) \rightarrow \gamma f_0(980)$ : the calculated amplitude  $A_{dipole}^{(calc)}$  versus the experimental one  $A^{(exp)}$ .

The comparison of the data (58) to the calculated amplitude is shown in Fig. 9. We see that the calculated amplitude (59) is in a perfect agreement with data, when  $M_{f_0^{bare}} \simeq 750 - 800$  MeV, that is just inside the error bars given by the K-matrix analysis [1].

## 6 Pion-pion spectrum in $\phi(1020) \rightarrow \gamma\pi\pi$

The  $f_0(980)$  resonance is seen in the reaction  $\phi(1020) \rightarrow \gamma\pi\pi$  as a peak at the edge of the  $\pi\pi$  spectrum. So it is rather enlightening to calculate the  $\pi\pi$  spectrum to be sure that its description agrees both with the quark model calculation of the form factor  $F_{\phi(1020) \rightarrow \gamma f_0(980)}$  and threshold theorem (cross section tending to zero as  $\omega^3$  at  $\omega \rightarrow 0$ , where  $\omega = m_\phi - M_{\pi\pi}$ ).

Partial cross section of the decay  $\phi(1020) \rightarrow \gamma\pi^0\pi^0$  is given by the following formula:

$$\begin{aligned} \frac{d\Gamma_{\phi(1020) \rightarrow \gamma\pi^0\pi^0}}{dM_{\pi\pi}} &= \frac{1}{3} \Gamma_{\phi(1020) \rightarrow \gamma f_0(980)} \frac{m_\phi^2 - M_{\pi\pi}^2}{m_\phi^2 - m_{f_0}^2} \times \\ &\times \frac{2M_{\pi\pi}}{\pi} \rho_{\pi\pi} \left| \frac{g_\pi}{M_0^2 - M_{\pi\pi}^2 - ig_\pi^2 \rho_{\pi\pi} - ig_K^2 \rho_{K\bar{K}}} + B(M_{\pi\pi}^2) \right|^2. \end{aligned} \quad (60)$$

The factor  $1/3$  in front of the right-hand side (60) is associated with the  $\pi^0\pi^0$  channel:  $\Gamma_{\phi(1020) \rightarrow \gamma\pi^0\pi^0} = \frac{1}{3} \Gamma_{\phi(1020) \rightarrow \gamma\pi\pi}$ . Here for the description of the  $f_0(980)$  we use the Flatté formula [24] with the phase space factors

$$\rho_{\pi\pi} = \frac{1}{M_0} \sqrt{M_{\pi\pi}^2 - 4m_\pi^2}, \quad \rho_{K\bar{K}} = \frac{1}{M_0} \sqrt{M_{\pi\pi}^2 - 4m_K^2}. \quad (61)$$

At  $M_{\pi\pi}^2 < 4m_K^2$  one should replace  $\sqrt{M_{\pi\pi}^2 - 4m_K^2} \rightarrow i\sqrt{4m_K^2 - M_{\pi\pi}^2}$ . In line with [22, 23, 25], we use the Flatté formula with the parameters:

$$g_\pi^2 = 0.12 \text{ GeV}^2, \quad g_K^2 = 0.27 \text{ GeV}^2, \quad M_0 = 0.975 \text{ GeV}. \quad (62)$$

The threshold theorem requires

$$\left[ \frac{g_\pi}{M_0^2 - M_{\pi\pi}^2 - ig_\pi^2 \rho_{\pi\pi} - ig_K^2 \rho_{K\bar{K}}} + B(M_{\pi\pi}^2) \right]_{M_{\pi\pi} \rightarrow m_\phi} \sim (M_{\pi\pi} - m_\phi), \quad (63)$$

that gives a constraint for the background term  $B(M_{\pi\pi}^2)$ . The term  $B(M_{\pi\pi}^2)$  is parametrized in the form:

$$B(M_{\pi\pi}^2) = C \left[ 1 + a(M_{\pi\pi}^2 - m_\phi^2) \right] \exp \left[ -\frac{m_\phi^2 - M_{\pi\pi}^2}{\mu^2} \right], \quad (64)$$

and the parameter  $C$  is fixed by the constraint:

$$\left[ \frac{g_\pi}{M_0^2 - M_{\pi\pi}^2 - ig_\pi^2 \rho_{\pi\pi} - ig_K^2 \rho_{K\bar{K}}} + C \right]_{M_{\pi\pi} = m_\phi} = 0. \quad (65)$$

Fitting to the  $\pi^0\pi^0$  spectrum [22], see Fig. 10a, we have the following values for other parameters:

$$\frac{1}{a} = -0.2 \text{ GeV}^2, \quad \mu = 0.388 \text{ GeV}. \quad (66)$$

For  $\Gamma_{\phi(1020) \rightarrow \gamma f_0(980)}$  entering (60) we have used  $A_{\phi(1020) \rightarrow \gamma f_0(980)} = 0.13 \text{ GeV}$  that satisfies both (58) and (59).

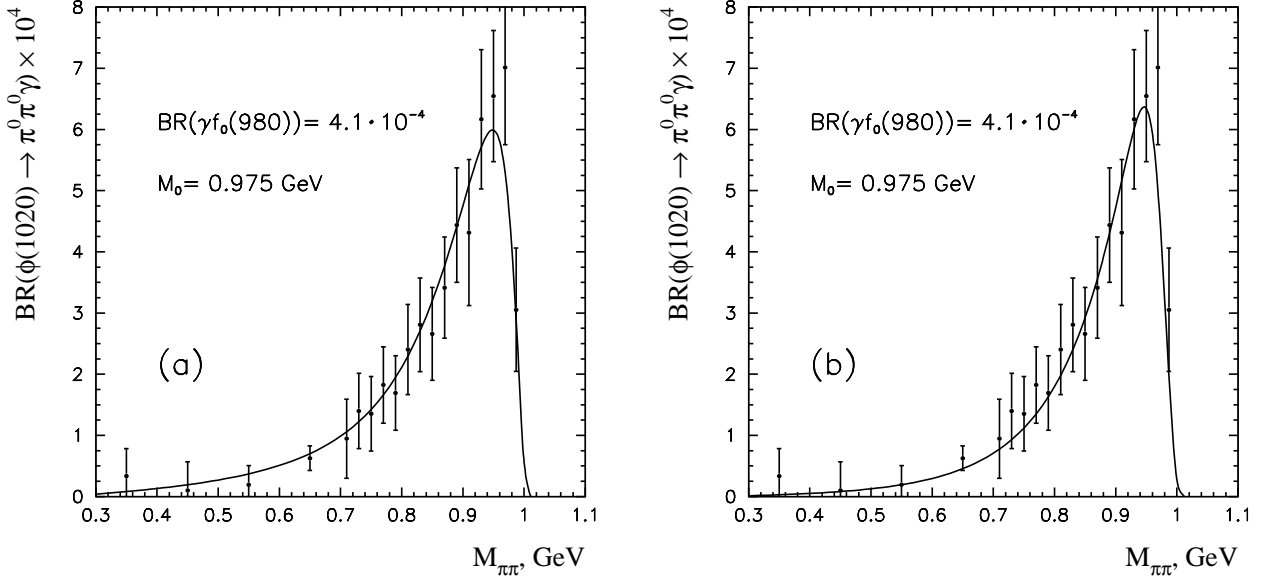


Figure 10: The  $\pi\pi$  spectrum of the reaction  $\phi(1020) \rightarrow \gamma\pi\pi$  calculated with the Flatté formula (a) and Eq. (68) (b).

The Flatté formula gives us rather rough description of the  $\pi\pi$ -amplitude around the  $f_0(980)$  resonance. More precise description may be obtained by using in addition the non-zero transition length for  $\pi\pi \rightarrow K\bar{K}$  [21]. For this case, we have the formulae analogous to Eq. (60), after replacing the resonance factor

$$\frac{g_\pi}{M_0^2 - M_{\pi\pi}^2 - ig_\pi^2 \rho_{\pi\pi} - ig_K^2 \rho_{K\bar{K}}} \quad (67)$$

by the following one:

$$\frac{g_\pi + i\rho_{K\bar{K}} g_K f}{M_0^2 - M_{\pi\pi}^2 - ig_\pi^2 \rho_{\pi\pi} - i\rho_{K\bar{K}} [g_K^2 + i\rho_{\pi\pi} (2g_\pi g_K f + f^2 (m_0^2 - s))]} \quad (68)$$

The parameters found in [21] are equal to:

$$\begin{aligned} g_\pi &= 0.386 \text{ GeV}, & g_K &= 0.447 \text{ GeV}, \\ M_0 &= 0.975 \text{ GeV}, & f &= 0.516. \end{aligned} \quad (69)$$

The transition length  $a_{\pi\pi \rightarrow K\bar{K}}$  is determined by the parameter  $f$  as follows:  $a_{\pi\pi \rightarrow K\bar{K}} = 2f/M_0$ .

The description of the  $\pi^0\pi^0$  spectra [22] within the resonance formulae (68) is demonstrated in Fig. 10b. In this fit we have the following parameters for  $B(M_{\pi\pi}^2)$ :

$$a = 0, \quad \mu = 0.507 \text{ GeV}. \quad (70)$$

In this variant of the fitting to spectra we also used  $A_{\phi(1020) \rightarrow \gamma f_0(980)} = 0.13 \text{ GeV}$ .

Let us emphasize that the visible width of the  $f_0(980)$  signal in the  $\pi\pi$  spectrum is comparatively large,  $\sim 150$  MeV, that is related to an essential contribution of the second pole at  $960 - i200$  MeV.

## 7 The additive quark model, does it work?

Let us point to the two aspects of this question. One is the problem of the applicability of the additive quark model to the production of the resonance  $f_0(980)$ , another one is the production of the bare state  $f_0^{bare}(700 \pm 100)$ .

### 1. Process $\phi(1020) \rightarrow \gamma f_0^{bare}(700 \pm 100)$

The additive quark model describes well the production of the bare state  $f_0^{bare}(700 \pm 100)$ , provided its mass is in the region  $750-800$  MeV. To see it, consider Eq. (38) for  $F_{\mu\alpha}^{\phi \rightarrow \gamma f_0}$  (dipole), or Eq. (17), where exponential representation of the quark wave functions is used. Formula (17) takes into account both the additive quark model processes and photon emission by the charge-exchange current, while Eq. (16) gives us the triangle-diagram contribution within additive quark model. The contribution of the charge-exchange current is small, when

$$m_s[m_\phi - M_{f_0^{bare}}] \simeq \frac{1}{b_\phi} . \quad (71)$$

At  $m_s = 0.5$  GeV and  $b_\phi = 10$  GeV $^{-2}$  the equality (71) is almost fulfilled, when  $M_{f_0^{bare}} \simeq 0.8$  GeV. Such a magnitude is allowed by the  $K$ -matrix fit [1], which gives  $M_{f_0^{bare}} = 0.7 \pm 0.1$  GeV.

However, let us emphasize that the error bars  $\pm 0.1$  GeV are rather large in the difference  $(m_\phi - M_{f_0^{bare}})$ : with the lower possible limit  $M_{f_0^{bare}} = 0.6$  GeV we face a two-times disagreement in Eq. (71). Still, one may hardly hope that the  $K$ -matrix analysis of the  $00^{++}$  wave would provide us with a tighter restriction for the mass of this bare state, since a large uncertainty in the definition of  $M_{f_0^{bare}}$  is not related to the data accuracy but to the problem of the light  $\sigma$  meson existence, see the discussions in [5, 26, 27, 28] and references therein.

The use of  $F_{\mu\alpha}^{\phi \rightarrow \gamma f_0}$  (additive), Eq. (16), for the calculation of  $A_{\phi(1020) \rightarrow \gamma f_0(980)}^{(calc)}$  results in the agreement with experimental data. Thus we have:

$$A_{\phi(1020) \rightarrow \gamma f_0(980)}^{(calc)}(\text{additive}) \simeq (0.58 \pm 0.04) \cdot \sqrt{W_{q\bar{q}}[f_0^{bare}(700)]} Z_{\phi \rightarrow \gamma f_0}^{(s\bar{s})} \times \times \frac{2^{7/2}}{\sqrt{3}} \frac{b_\phi^{3/4} b_{f_0}^{5/4}}{(b_\phi + b_{f_0})^{5/2}} . \quad (72)$$

In Fig. 11, one can see  $A_{\phi(1020) \rightarrow \gamma f_0(980)}^{(calc)}(\text{additive})$  versus  $A_{\phi(1020) \rightarrow \gamma f_0(980)}^{(exp)}$ : there is a good agreement with data.

The existence of two characteristic sizes in a hadron, namely, hadronic radius and that of constituent quark, may be the reason why the contribution of the charge-exchange current is small in the reaction  $\phi(1020) \rightarrow \gamma f_0^{bare}(700)$ . Relatively small radius of the constituent quark assumes that charge-exchange interaction  $s\bar{s} \rightarrow gg \rightarrow n\bar{n}$  is a short-range one, that causes a smallness of the second term in the right-hand side (35).

The hadronic size is defined by the confinement radius  $R_h \sim R_{\text{confinement}}$ , which is of the order of 1 fm for light hadrons. The constituent quark size,  $r_q$ , is much smaller, it is defined, as one may believe, by relatively large mass of the soft gluon (experimental data [29] and lattice

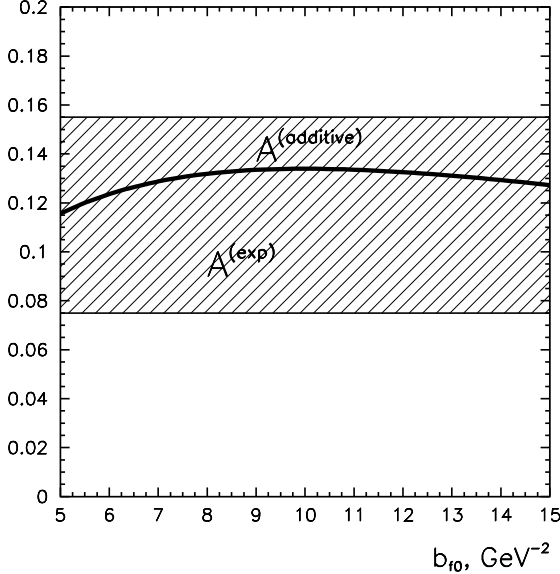


Figure 11: The additive quark model amplitude for  $\phi(1020) \rightarrow \gamma f_0(980)$ , Eq. (72), versus  $A_{\phi(1020) \rightarrow \gamma f_0(980)}^{(exp)}$ .

calculations [30] give us  $m_g \sim 700 - 1000$  MeV). So we get  $r_q^2/R_h^2 \sim (0.1 - 0.2)$ , the same value follows from the analysis of soft hadron collisions, see [15, 31] and references therein.

## 2. Process $\phi(1020) \rightarrow \gamma f_0(980)$

The two sizes,  $r_q^2$  and  $R_h^2$ , being accepted, the additive quark model contribution dominates the reaction  $\phi(1020) \rightarrow \gamma f_0(980)$  too, thus allowing direct use of the triangle diagram of Fig. 1a for the calculation of this process. Such calculations were performed in [17], revealing resonable agreement with data. Once again it should be emphasized that the triange diagram contribution does not have a particular smallness related to a deceptive proximity of  $\phi(1020)$  and  $f_0(980)$ . Besides, as was explained above, the poles associated with these resonances are separated from each other in the complex- $M$  plane in non-small distances in the hadronic scale.

In the literature there exist rather opposite statements about the possibility to describe the reaction  $\phi(1020) \rightarrow \gamma f_0(980)$  within the frame of the hypothesis of the  $q\bar{q}$  nature of  $f_0(980)$ . Using the QCD sum-rule technique the authors of [32] evaluated the rate of the decay  $\phi(1020) \rightarrow \gamma f_0(980)$ , with a fair agreement with data, supposing a sizeable  $s\bar{s}$  component in the  $f_0(980)$ .

The results of the calculation performed in [33] in the framework of the additive quark model do not agree with data on the reaction  $\phi(1020) \rightarrow \gamma f_0(980)$ . This calculation though similar to those of [16, 17] led to different result, so it would be instructive to compare model parameters used in these two approaches.

In [33] as well as [16, 17], the exponential parametrization of the wave function was used, however the slopes  $b_\phi$  and  $b_{f_0}$  in [33] were considerably smaller (constituent quark masses are smaller too). In [33],  $b_{s\bar{s}} = 2.9$  GeV $^{-2}$  and  $b_{u\bar{u}} = b_{d\bar{d}} = 3.7$  GeV $^{-2}$  ( $m_u = m_d = 220$  MeV,

$m_s = 450$  MeV), while in [16, 17]  $b_\phi \simeq 10$  GeV $^{-2}$  and  $b_\phi \sim b_{f_0}$  ( $m_u = m_d = 350$  MeV,  $m_s = 500$  MeV). Besides, in [33] the scheme of the mixing of  $f_0$ -states was used that was suggested in [34, 35], where the transitions  $f_0^{bare} \rightarrow$  *real mesons* were not accounted for. Still, as was emphasized above (Section 5.2), just the transitions  $f_0^{bare} \rightarrow \pi\pi, K\bar{K}, \eta\eta, \pi\pi\pi\pi$  afford the final disposition of poles in the complex plane, for they are responsible for the resonance mass shift of the order of 100 MeV, see Fig. 5.

In our opinion, the failure of the  $q\bar{q}$  model demonstrated in [33] can testify only the fact that not any model enables the description of radiative decays. The  $q\bar{q}$  model should be based on the whole set of experimental data but not on the reproducing several levels of the lowest states.

## 8 Conclusion

Correct determination of the origin of  $f_0(980)$  is a key for understanding of the status of the light  $\sigma$  and classification of heavier mesons  $f_0(1300)$ ,  $f_0(1500)$ ,  $f_0(1750)$  and the broad state  $f_0(1200 - 1600)$ .

We have shown that experimental data on the reaction  $\phi(1020) \rightarrow \gamma f_0(980)$  do not contradict the suggestion about the dominance of the quark–antiquark component in the  $f_0(980)$ . However, as was emphasized in Introduction, the final conclusion about the origin of  $f_0(980)$  should be made on the basis of the whole availability of arguments, so let us enumerate them briefly.

1. There are data on the hadronic decays of the lowest mesons, and the most reliable information on scalar resonances is given by the  $K$ -matrix analysis. Summing up, one can state that, according to the  $K$ -matrix analysis [1], the lowest states  $f_0(980)$ ,  $f_0(1300)$ ,  $a_0(980)$ ,  $K_0(1430)$  are the descendants of bare mesons, which have created the  $1^3P_0$  multiplet. Because of that, all the decays, namely,

$$\begin{aligned} f_0(980) &\rightarrow \pi\pi, K\bar{K}, \\ f_0(1300) &\rightarrow \pi\pi, K\bar{K}, \eta\eta, \\ a_0(980) &\rightarrow K\bar{K}, \pi\eta, \\ K_0(1430) &\rightarrow K\pi, \end{aligned} \tag{73}$$

are described by two parameters only in the leading terms of the  $1/N_c$  expansion, which are the universal coupling constant and mixing angle for the  $n\bar{n}$  and  $s\bar{s}$  components in the scalar–isoscalar sector.

2. Another argument is the systematics of scalar states on linear trajectories on the  $(n, M^2)$ -plane. For scalar mesons the trajectories are shown in Fig. 12a — one can see that  $f_0(980)$  lays comfortably on linear trajectory, together with the other scalars. Such trajectories are formed not only for the scalar sector but also for all aggregate of data, see [4, 5], and all the trajectories are characterized by the universal slope.

Similar  $q\bar{q}$  trajectories exist in the  $(J, M^2)$ -plane too, and  $f_0(980)$  belongs to one of them.

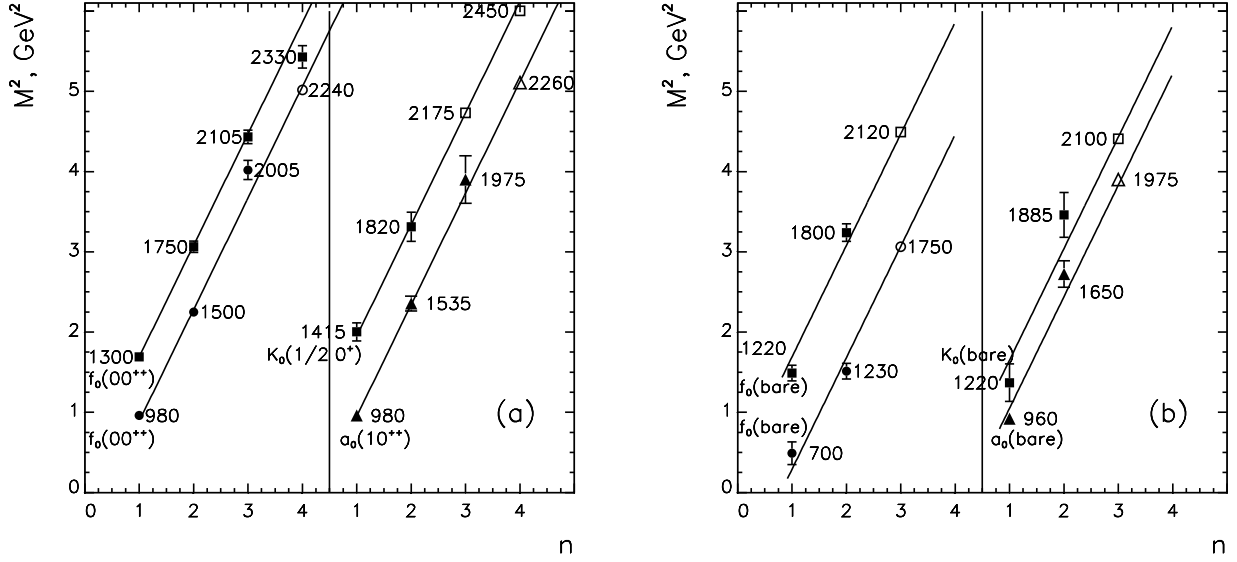


Figure 12: Linear trajectories on the  $(n, M^2)$  plane for bare states (a) and scalar resonances (b).

3. The alternative to the  $q\bar{q}$  system may be the four-quark  $q\bar{q}q\bar{q}$ , or molecular  $K\bar{K}$  structure [6, 7, 36, 37]. Such a nature of  $f_0(980)$  would mean that  $f_0(980)$  was loosely bound system but the experiment tells us that this is not so. The matter is that

- (i)  $f_0(980)$  is easily produced at large momenta transferred to the nucleon in the reaction  $\pi^- p \rightarrow f_0(980)n$  [38, 39],
- (ii)  $f_0(980)$  is produced in the  $Z^0$ -boson decays [40],
- (iii)  $f_0(980)$  is produced in central  $pp$  collisions at high energies [41].

Were the  $f_0(980)$  a loosely bound system, these processes would be suppressed.

4. The  $f_0(980)$  resonance is produced in hadronic decays of the  $D_s$  meson,  $D_s^+ \rightarrow \pi^+ f_0(980)$ , with the probability comparable with that for the transition  $D_s^+ \rightarrow \pi^+ \phi(1020)$  [42]. These two reactions are due to the weak decay of  $c$ -quark,  $c \rightarrow \pi^+ s$ ; as to  $f_0(980)$ , it is formed, like  $\phi(1020)$ , by the  $s\bar{s}$ -system in the transition  $s\bar{s} \rightarrow f_0(980)$ . The calculation of this process [43] shows us that the  $f_0(980)$  yield in the reaction  $D_s^+ \rightarrow \pi^+ f_0(980)$  can be reliably calculated under the assumption that  $f_0(980)$  is close to the  $q\bar{q}$  flavour octet.

The study of the  $D_s^+ \rightarrow \pi^+ f_0(980)$  decay by [44, 45, 46] also led to the conclusion about the  $s\bar{s}$  nature of  $f_0(980)$ .

5. Concerning radiative decays with the formation of  $f_0(980)$ , we see that the transition  $\phi(1020) \rightarrow \gamma f_0(980)$  can be well described within the approach of additive quark model, with the dominant  $q\bar{q}$  component in the  $f_0(980)$ . Another radiative decay,  $f_0(980) \rightarrow \gamma\gamma$ , partial width of which was measured [47], can be also treated in terms of the  $q\bar{q}$  structure of  $f_0(980)$  [16, 48]. The values of partial widths in both decays support the conclusion made in [1] that the flavour content of  $f_0(980)$  is close the octet one.

We thank Ya.I. Azimov, L.G. Dakhno, S.S. Gershtein, Yu.S. Kalashnikova, A.K. Likhoded, M.A. Matveev, D.I. Melikhov, and W.B. von Schlippe for helpful and stimulating discussions of problems involved. This work is supported by the RFBR Grant N 0102-17861. V.N.M. was supported in part by INTAS call 2000 project 587 and "Dynasty Foundation".

## Appendix A: Dipole emission of photon

To describe the interaction of composite system with electromagnetic field, we consider the full Hamiltonian:

$$\hat{H}(0) = \begin{vmatrix} \frac{1}{2m}k_1^2 + \frac{1}{2m}k_2^2 + U_{s\bar{s} \rightarrow s\bar{s}}(\mathbf{r}_1 - \mathbf{r}_2) & , & \hat{U}_{s\bar{s} \rightarrow gg}(\mathbf{r}_1 - \mathbf{r}_2) \\ U_{s\bar{s} \rightarrow gg}(\mathbf{r}_1 - \mathbf{r}_2) & , & \frac{1}{2m_g}k_1^2 + \frac{1}{2m_g}k_2^2 + U_{gg \rightarrow gg}(\mathbf{r}_1 - \mathbf{r}_2) \end{vmatrix}. \quad (74)$$

Here the coordinates ( $\mathbf{r}_a$ ) and momenta ( $\mathbf{k}_a = -i\nabla_a$ ) of the constituents are related to the characteristics of the relative movement, entering (31), as follows

$$\mathbf{r}_1 = \frac{1}{2}\mathbf{r} + \mathbf{R}, \quad \mathbf{r}_2 = -\frac{1}{2}\mathbf{r} + \mathbf{R}, \quad \mathbf{k}_1 = \frac{1}{2}\mathbf{k} + \mathbf{P}, \quad \mathbf{k}_2 = -\frac{1}{2}\mathbf{k} + \mathbf{P}. \quad (75)$$

The electromagnetic interaction is included by substituting in (74) as follows:

$$\begin{aligned} \mathbf{k}_1^2 &\rightarrow (\mathbf{k}_1 - e_1 \mathbf{A}(r_1))^2, & \mathbf{k}_2^2 &\rightarrow (\mathbf{k}_2 - e_2 \mathbf{A}(r_2))^2, \\ \hat{U}_{s\bar{s} \rightarrow gg}(\mathbf{r}_1 - \mathbf{r}_2) &\rightarrow \hat{U}_{s\bar{s} \rightarrow gg}(\mathbf{r}_1 - \mathbf{r}_2) \exp \left[ ie_1 \int_{-\infty}^{\mathbf{r}_1} dr'_\alpha A_\alpha(r') + ie_2 \int_{-\infty}^{\mathbf{r}_2} dr'_\alpha A_\alpha(r') \right], \end{aligned} \quad (76)$$

with  $e_1 = -e_2 = e_s$ . After that we obtain the gauge-invariant Hamiltonian  $\hat{H}(A)$ :

$$\hat{H}(\mathbf{A}) = \hat{\chi}^+ \hat{H}(\mathbf{A} + \nabla \chi) \hat{\chi}, \quad (77)$$

where  $\mathbf{A} + \nabla \chi$  means the following substitution:

$$\mathbf{A}(r_a) \rightarrow \mathbf{A}(r_a) + \nabla \chi(r_a), \quad (78)$$

and matrix  $\hat{\chi}$  reads:

$$\hat{\chi} = \begin{vmatrix} \exp[ie_s \chi(r_1) - ie_s \chi(r_2)] & , & 0 \\ 0 & , & 1 \end{vmatrix}. \quad (79)$$

For the transition  $\phi \rightarrow \gamma f_0$ , keeping the terms proportional to the  $s$ -quark charge,  $e_s$ , we have the following operator for the dipole emission:

$$\hat{d}_\alpha = \begin{vmatrix} 2(k_{1\alpha} - k_{2\alpha}) & , & i(r_{1\alpha} - r_{1\alpha}) \hat{U}_{s\bar{s} \rightarrow gg}(\mathbf{r}_1 - \mathbf{r}_2) \\ -i(r_{1\alpha} - r_{1\alpha}) \hat{U}_{s\bar{s} \rightarrow gg}(\mathbf{r}_1 - \mathbf{r}_2) & , & 0 \end{vmatrix}. \quad (80)$$

There exist other mechanisms of the photon emission which, being beyond the additive quark model, lead us to the dipole formula for  $V \rightarrow \gamma S$  transition, an example is given by **(LS)**-interaction in the quark-antiquark component [9, 10, 49]. The short-range **(LS)**-interaction in the  $q\bar{q}$  systems, was discussed in [50, 51] as a source of the nonet splitting. Actually the point-like **(LS)**-interaction gives  $(v/c)$ -corrections to the non-relativistic approach. In the relativistic quark model approaches based on the Bethe-Salpeter equation, the gluon-exchange forces result in similar nonet splitting as for the **(LS)**-interaction, for example, see [52].

## References

- [1] V.V. Anisovich and A.V. Sarantsev, Eur. Phys. J. A **16**, 229 (2003).
- [2] V.V. Anisovich, A.A. Kondashov, Yu.D. Prokoshkin, S.A. Sadovsky and A.V. Sarantsev, Yad. Fiz. **60**, 1489 (2000) [Physics of Atomic Nuclei **60**, 1410 (2000)].
- [3] V.V. Anisovich and A.V. Sarantsev, Phys. Lett. **B382**, 429 (1996);  
V.V. Anisovich, Yu.D. Prokoshkin and A.V. Sarantsev, Phys. Lett. **B389**, 388 (1996).
- [4] A.V. Anisovich, V.V. Anisovich and A.V. Sarantsev, Phys. Rev. D **62**:051502 (2000);  
V.V. Anisovich, hep-ph/0310165.
- [5] V.V. Anisovich, UFN **174**, 49 (2004); hep-ph/0208123 v3.
- [6] R.L. Jaffe, Phys. Rev. D **15**, 267 (1977).
- [7] J. Weinshtein and N. Isgur, Phys. Rev. D **41**, 2236 (1990).
- [8] F.E. Close et al., Phys. Lett. **B319**, 291 (1993).
- [9] N. Byers and R. MacClary, Phys. Rev. D **28**, 1692 (1983).
- [10] A. LeYaouanc, L. Oliver, O. Pene, and J.C. Raynal, Z. Phys. **C40**, 77 (1988).
- [11] A.J.F. Siegert, Phys. Rev. **52**, 787 (1937).
- [12] V.V. Anisovich and M.A. Matveev, hep-ph/0303119 (2003).
- [13] S. Malvezzi, "Dalitz plot analysis of  $D_s^+$  and  $D^+$  decay to  $\pi^+\pi^+\pi^-$  using the K-matrix formalism", Talk given at "Hadron-03", Aschafensburg, Germany, 30 August-6 September 2003.
- [14] A.V. Anisovich and V.V. Anisovich, Phys. Lett. **B467**, 289 (1999).
- [15] V.V. Anisovich, M.N. Kobrinsky, J. Nyiri and Yu.M. Shabelski, "Quark Model and High Energy Collisions", 2nd Edition, World Scientific, Singapore, 2004.
- [16] A.V. Anisovich, V.V. Anisovich and V.A. Nikonov, Eur. Phys. J. A **12**, 103 (2001).
- [17] A.V. Anisovich, V.V. Anisovich, V.N. Markov and V.A. Nikonov, Yad. Fiz. **65**, 523 (2002);  
[Phys. Atom. Nuclei **65**, 497 (2002)].
- [18] A.V. Anisovich, V.V. Anisovich and V.A. Nikonov, hep-ph/0305216 (2003).
- [19] G.S. Bali et al., Phys. Lett. **B309**, 378 (1993);  
J. Sexton, A. Vaccarino and D. Weingarten, Phys. Rev. Lett. **75** 4563 (1995);  
C.J. Morningstar and M. Peardon, Phys. Rev. D **56**, 4043 (1997).
- [20] D.E. Groom et al. (PDG), Eur. Phys. J. C **15**, 1 (2000).

- [21] V.V. Anisovich, V.A. Nikonov and A.V. Sarantsev, *Yad. Fiz.* **65**, 1583 (2002); [*Phys. Atom. Nuclei* **65**, 1545 (2002)];  
*Yad. Fiz.* **66**, 772 (2003); [*Phys. Atom. Nuclei*, **66**, 741 (2003)].
- [22] M.N. Achasov et al., *Phis. Lett.* **B485**, 349 (2000).
- [23] R.R. Akhmetshin et al., *Phys. Lett.* **B462**, 380 (1999).
- [24] S.M. Flatté, *Phys. Lett.* **B63**, 224 (1976).
- [25] A.V. Sarantsev, private communication.
- [26] S.F. Tuan, hep-ph/0303248.
- [27] E. van Beveren et al., *Mod. Phys. Lett.* **A17**, 1673 (2002).
- [28] W. Ochs and P. Minkowski, *Nucl. Phys. Proc. Suppl.* **121**, 123 (2003).
- [29] G. Parisi and R. Petronzio, *Phys. Lett.* **B94**, 51 (1980);  
M. Consoli and J.H. Field, *Phys. Rev.* **D49**, 1293 (1994).
- [30] D.B. Leinweber et al., *Phys. Rev.* **D58**:031501 (1998).
- [31] L.G. Dakhno and V.A. Nikonov, *Eur. Phys. J.* **A5**, 209 (1999).
- [32] F. De Fazio and M.R. Pennington, *Phys. Lett.* **B521**, 15 (2001).
- [33] M.A. DeWitt, H.M. Choi and C.R. Ji, *Phys. Rev. D* **68**: 054026 (2003).
- [34] W. Lee and D. Weingarten, *Phys. Rev. D* **61**: 014015 (1999).
- [35] F.E. Close and A. Kirk, *Eur. Phys. J.* **C21**, 531 (2001).
- [36] F.E. Close, *Int. J. Mod. Phys.* **A17**, 3239 (2002).
- [37] N.N. Achasov, *AIP Conf. Proc.* **619**, 112 (2002).
- [38] D. Alde et al., *Zeit. Phys. C* **66**, 375 (1995);  
Yu.D. Prokoshkin et al., *Physics – Doklady* **342**, 473 (1995).
- [39] J. Gunter et al. (E852 Collaboration), *Phys. Rev. D* **64**:07003 (2001).
- [40] K. Ackerstaff et al., *Eur. Phys. J.* **C4**, 19 (1998).
- [41] D. Barberis et al., *Phys. Lett.* **B453**, 325 (1999).
- [42] E.M. Aitola et al., *Phys. Rev. Lett.* **86**, 765 (2001).
- [43] V.V. Anisovich, L.G. Dakhno and V.A. Nikonov, hep-ph/0302137.
- [44] P. Minkowski and W. Ochs, *Nucl. Phys. Proc. Suppl.* **121**, 119 (2003).

- [45] F. Kleefeld et al., Phys. Rev. D **66**:034007 (2002).
- [46] A. Deandrea et al., Phys. Lett. **B502**, 79 (2001).
- [47] M. Boglione and M.R. Pennington, Eur. Phys. J. C **9**, 11 (1999).
- [48] A.V. Anisovich, V.V. Anisovich, M.A. Matveev and V.A. Nikonov, Yad. Fiz. **66**, 946 (2003); [Phys. Atom. Nuclei, **66**, 914 (2003)].
- [49] Yu.S. Kalashnikova, private communication.
- [50] Ya.B. Zeldovich and A.D. Sakharov, Yad. Fiz. **4**, 395 (1966); [Sov. J. Nucl. Phys. **4**, 283 (1967)].
- [51] A. de Rujula, H. Georgi and S.L. Glashow, Phys. Rev. D **12**, 147 (1975).
- [52] R. Ricken, M. Koll, D. Merten, B.C. Metsch and H.R. Petry, Eur. Phys. J. A**9**, 221 (2000).